Journal of Human Evolution 181 (2023) 103395

Contents lists available at ScienceDirect

Journal of Human Evolution

journal homepage: www.elsevier.com/locate/jhevol

Early euprimates already had a diverse locomotor repertoire: Evidence from ankle bone morphology

Oriol Monclús-Gonzalo [a, 1], David M. Alba [a], Anaïs Duhamel [b], Anne-Claire Fabre [c, d, e, *, 1], Judit Marigó [f, a, *, 1]

[a] Institut Català de Paleontologia Miquel Crusafont, Universitat Autònoma de Barcelona, Edifici ICTA-ICP, c/ Columnes s/n, 08193 Cerdanyola del Vallès, Barcelona, Spain
[b] University of Lyon, ENSL, CNRS, LGL-TPE, Villeurbanne 69622, France
[c] Naturhistorisches Museum Bern, 3005 Bern, Switzerland
[d] Institute of Ecology and Evolution, University of Bern, 3012 Bern, Switzerland
[e] Life Sciences Department, Vertebrates Division, Natural History Museum, London SW7 5BD, UK
[f] Universitat Autònoma de Barcelona, Departament de Geologia, 08193 Cerdanyola del Vallès, Barcelona, Spain

ARTICLE INFO

Article history:
Received 9 August 2022
Accepted 8 May 2023
Available online 13 June 2023

Keywords:
Early euprimates
Locomotor repertoire
Geometric morphometrics
Functional morphology
Paleogene
Navicular

ABSTRACT

The morphological adaptations of euprimates have been linked to their origin and early evolution in an arboreal environment. However, the ancestral and early locomotor repertoire of this group remains contentious. Although some tarsal bones like the astragalus and the calcaneus have been thoroughly studied, the navicular remains poorly studied despite its potential implications for foot mobility. Here, we evaluate early euprimate locomotion by assessing the shape of the navicular—an important component of the midtarsal region of the foot—using three-dimensional geometric morphometrics in relation to quantified locomotor repertoire in a wide data set of extant primates. We also reconstruct the locomotor repertoire of representatives of the major early primate lineages with a novel phylogenetically informed discriminant analysis and characterize the changes that occurred in the navicular during the archaic primate–euprimate transition. To do so, we included in our study an extensive sample of naviculars (36 specimens) belonging to different species of adapiforms, omomyiforms, and plesiadapiforms. Our results indicate that navicular shape embeds a strong functional signal, allowing us to infer the type of locomotion of extinct primates. We demonstrate that early euprimates displayed a diverse locomotor behavior, although they did not reach the level of specialization of some living forms. Finally, we show that the navicular bone experienced substantial reorganization throughout the archaic primate–euprimate transition, supporting the major functional role of the tarsus during early primate evolution. This study demonstrates that navicular shape can be used as a reliable proxy for primate locomotor behavior. In addition, it sheds light on the diverse locomotor behavior of early primates as well as on the archaic primate–euprimate transition, which involved profound morphological changes within the tarsus, including the navicular bone.

1. Introduction

Extant primates are very diverse in body size (from ~30 g in mouse lemurs to 200 kg in male gorillas) and locomotor behavior, including arboreal and terrestrial quadrupedalism, vertical clinging and leaping (VCL), climbing and suspensory behaviors, and terrestrial bipedalism, among others (Oxnard et al., 1990; Hunt et al., 1996; Fleagle, 2013). Several evolutionary scenarios have been proposed to explain the origin and evolution of primates of modern aspect (or euprimate, sensu Hoffstetter, 1977) locomotor diversity from an adaptive viewpoint, but they remain highly debated (Napier and Walker, 1967; Walker, 1974; Cartmill, 1974, 1992; Szalay and Dagosto, 1980; Dagosto, 1988, 2007; Rasmussen, 1990; Sussman, 1991). The early adaptive radiation of euprimates (adapiforms and omomyiforms) has been extensively investigated based on postcranial remains, especially ankle bones such as the

* Corresponding authors.
E-mail addresses: fabreac@gmail.com (A.-C. Fabre), judit.marigo@uab.cat (J. Marigó).
[1] O.M.G, A.-C.F., and J.M. contributed equally to this work.

https://doi.org/10.1016/j.jhevol.2023.103395

calcaneus, astragalus, and navicular, as they are well represented in the fossil record and considered to be good proxies for locomotor habits among primates (e.g., Decker and Szalay, 1974; Szalay and Decker, 1974; Conroy and Rose, 1983; Rose and Walker, 1985; Covert, 1988; Gebo et al., 1991, 2015; Moyà-Solà et al., 2012; Boyer et al., 2013, 2015, 2017a; Llera Martín et al., 2022). The morphology of these bones suggests that the archaic primate–euprimate transition was characterized by a substantial reorganization of the foot (Dagosto, 1988, 2007). Nonetheless, an integrative study relating foot bone morphology with quantified locomotor data in a broad sample of living and extinct primates is currently missing.

Among early euprimates, basal omomyiforms have been proposed to be more active and prone to leaping than basal adapiforms (Walker, 1974; Gebo, 1988; Rose, 1994; Boyer et al., 2013). However, differences in body size between the members of these groups have hindered the interpretation of their morphological differences, as adapiforms (except for some small forms such as *Anchomomys frontanyensis*) are substantially larger than most omomyiforms (Rose, 1994), although within the latter group there are also larger-bodied species (Dunn et al., 2006; Dunn, 2010). For this reason, it has been suggested that some morphological differences between these groups might simply reflect size-scaling (allometric) effects instead of fundamental differences in locomotor behavior, although body mass and locomotor behavior are functionally interwoven (Walker, 1974). Furthermore, for biomechanical reasons, foot type has also been proposed as an important factor influencing tarsal morphology (Morton, 1924; Moyà-Solà et al., 2012). Foot types differ with respect to the location of the fulcrum, which is defined as the position in which the lever (in this case, the foot) pivots (Morton, 1924). Anthropoids and most nonprimate mammals have a metatarsi-fulcrumating foot, with the fulcrum placed on the heads of the metatarsals, associated with an increased load arm (Morton, 1924). In contrast, extant strepsirrhines and tarsiers have a tarsi-fulcrumating foot, where the fulcrum is located on the distal tarsal bones; this provides them increased grasping abilities but results in a reduced load arm, which is compensated by the elongation of the tarsus, especially the calcaneus and the navicular (Moyà-Solà et al., 2012). In addition, indriids are specialized VCLs that depart from the tarsi-fulcrumating condition, being described as 'tarsi-rotators' because their foot displays a greater range of inversion–eversion and acts solely as a force transducer instead of as a propulsive lever (Demes et al., 1996; Ankel-Simons, 2007). Moreover, they possess a derived adductor grasping mode (sensu Gebo, 1985; Gebo and Dagosto, 1988) characterized by an enhanced grasping action of the hallux and the second digit that enables the exploitation of the vertical support niche despite their large body size compared to other vertical clingers and leapers.

The functional morphology of the tarsus has been extensively studied for the calcaneus and astragalus of extinct primates (e.g., Decker and Szalay, 1974; Szalay and Decker, 1974; Lewis, 1980a,b; Godinot and Dagosto, 1983; Dagosto, 1988, 2007; Gebo, 1988; Gebo et al., 2000, 2001, 2012, 2015; Seiffert and Simons, 2001; Dunn et al., 2006; Dagosto et al., 2010; Dunn, 2010; Marivaux et al., 2010, 2011; Moyà-Solà et al., 2012; Boyer et al., 2013, 2015, 2017a, 2019; Gladman et al., 2013; Chester et al., 2015; Seiffert et al., 2015; Marigó et al., 2016; Yapuncich et al., 2017, 2019). These two bones account for the 31% and 38% of the fossil primate pedal remains preserved in the fossil record, respectively, indicating a strong bias toward their study compared with other foot elements (Yapuncich et al., 2022). They have been the most informative for our understanding of foot function, as they present several traits related to pedal grasping, load transmission, and degree of movements at the crural, subtalar, and transverse tarsal joints (Su and Zeiniger, 2022), allowing us to produce strong inferences about the locomotor behavior of extinct species. In contrast, the navicular remains comparatively poorly studied despite being important for midfoot mobility as an intermediate between the astragalus and the distal tarsals and metatarsals (Lewis, 1980b; Su and Zeiniger, 2022). Only a handful of studies have investigated the functional signal of the navicular (Covert, 1988; Dagosto, 1988, 2007; Gebo et al., 1991; Anemone and Covert, 2000; Dunn, 2010; Rose et al., 2011; Marigó et al., 2020), and none have used a geometric morphometrics approach, quantified locomotor data, or phylogenetic comparative methods. Differences in proximodistal elongation as well as in the morphology of the navicular facets among extant taxa with varied locomotor behaviors suggest that this bone may be useful for inferring the locomotor behavior of extinct primates and, hence, might provide additional insight into the reconstruction of the ancestral euprimate morphotype from an adaptive viewpoint.

We aim to investigate the evolution and diversification of the locomotor behavior of early euprimates. To do so, we use a three-dimensional (3D) geometric morphometric approach focused on the navicular and based on a large sample of extant and extinct species. These include representatives of the plesiadapiforms, as they are considered an early paraphyletic radiation of stem primates (Bloch et al., 2007; Silcox et al., 2015, 2017). We generated a novel data set including representatives of living lemuriforms and noncatarrhine haplorrhines, as well as a large sample of early primates from the Paleocene and Eocene (plesiadapiforms, adapiforms, and omomyiforms). We hypothesize that navicular morphology is functionally linked to the locomotor behavior of primates. Specifically, we predict that navicular shape (quantified by means of a 3D geometric morphometrics approach) is a reliable predictor of the locomotor repertoire of extant primates and, thus, can be used to infer the locomotion of extinct primate species for which this bone has been recovered. With regards to early euprimates, we hypothesize that their locomotor repertoire was already diverse early on in their evolution as they rapidly diversified in the arboreal niche, exploring different ecological strategies within the arboreal milieu. Notwithstanding, we predict that their locomotor adaptations were less specialized than the ones present in some extant species. Finally, we hypothesize that the locomotor mode played a critical role during the archaic primate–euprimate transition, leading to substantial morphological changes in the foot anatomy that can be traced on the navicular bone.

2. Materials and methods

2.1. Sample composition, data collection, and phylogenetic tree

The analyzed sample is composed of 121 naviculars belonging to 46 extant and 17 extinct primate species (alongside one specimen attributed to Omomyidae indet. [UCMP V 134984]). The extant taxa represent nearly the entire genus diversity of strepsirrhines (cheirogaleids: $n = 8$; galagids: $n = 2$; indriids: $n = 8$; lemurids: $n = 15$; lorisids: $n = 10$; daubentoniids: $n = 5$; and lepilemurids: $n = 2$) and a representative sample of extant noncatarrhine haplorrhines (atelids: $n = 10$; callitrichids: $n = 10$; cebids: $n = 5$; pitheciids: $n = 9$; and tarsiids: $n = 1$). Due to the semi(terrestrial) locomotor behavior of several catarrhine species, which is not adequate for comparison with early euprimates, this group has not been included in the sample. The extinct taxa correspond to 13 omomyiforms, 19 adapiforms, and four plesiadapiforms. The 3D models of all specimens were downloaded from the online repository MorphoSource (www.MorphoSource.org; Boyer et al., 2017b). The complete list of specimens analyzed is provided in Supplementary Online Material (SOM) Table S1, the list of living species and their locomotor data in SOM Table S2, and the list of extinct species in SOM Table S3.

A phylogenetic tree (SOM Fig. S1) comprising all extant primates in our study was downloaded from the 10kTrees Project v. 3 (Arnold et al., 2010). The criteria used to place the extinct taxa are explained in SOM S1. Unless otherwise stated, all analyses were performed in R v. 4.2.2 (R Core Team, 2022), and the alpha level of significance was set at $p < 0.05$.

2.2. Quantification of shape, impact of size, and navicular shape variation

Quantification of shape using three-dimensional geometric morphometrics To accurately depict navicular shape, a series of 16 homologous anatomical landmarks (Fig. 1; Table 1) was placed on the 3D surface of each specimen using the software Landmark v. 3.0.0.6 (Wiley, 2006). For those specimens belonging to the left foot, a mirroring of the mesh was performed before placing the landmarks in order to have the same orientation for all specimens. A generalized Procrustes analysis was carried out with the function 'gpagen' of the package geomorph v. 4.0.3 (Adams and Otárola-Castillo, 2013) to obtain the Procrustes shape coordinates (Rohlf and Slice, 1990; Mitteroecker and Gunz, 2009). A mean shape was calculated for each species, and species means were used as input in all further analyses.

Impact of size on navicular shape To assess the impact of navicular size on navicular shape in the analyzed sample, we first examined the correlation between navicular size and body mass (SOM Fig. S2). After that, we computed a series of allometric regressions of species-mean Procrustes shape coordinates vs. $\log_{10}$-transformed centroid size (CS; Goodall, 1991) in the entire sample and two subsets: only euprimates (excluding plesiadapiforms) and euprimates except for the small vertical clingers and leapers (*Tarsius spectrum*, *Galago moholi*, and *Sciurocheirus alleni*). We fitted a multivariate phylogenetic linear model with a Pagel's lambda by penalized likelihood using the 'mvgls' function of the package mvMORPH v. 1.1.6 (Clavel et al., 2015; Clavel and Morlon, 2020). A penalized-likelihood approach is a modern formulation of the regularization/shrinkage approaches, which are commonly used to constrain the estimates of parameters such as the maximum likelihood error, to address analyses in which the number of variables exceed the sample number (Clavel et al., 2019). Next, we tested for significant correlation between shape and centroid size using the function 'manova.gls'.

Navicular shape variation To assess navicular shape variation across the sample, a principal component analysis (PCA) was performed using the species-mean Procrustes shape coordinates. The phylogeny was plotted along with the results of the PCA, building a phylomorphospace using the function 'phylomorphospace' of the package phytools v. 0.7–20 (Revell, 2012).

2.3. Covariation between navicular shape and locomotion in extant euprimate species

To test the correlation between navicular shape and locomotor behavior, a quantified locomotor data set was compiled from the available literature. To assemble this data set, six different locomotor categories were used, following several field studies as well as the descriptions for standardized primate locomotor and postural modes presented by Hunt et al. (1996): quadrupedalism (Q), leaping (L), climbing (C), suspension (S), bridging (B), and scrambling/clambering (S/C; see SOM S1 for further details). We next performed a PCA to assess if the locomotor categories described in SOM Table S2 were suitable for describing the locomotor repertoire described in the field studies from which the locomotor percentages were retrieved (SOM Fig. S3).

A two-block partial least squares (2B-PLS) analysis (Rohlf and Corti, 2000) was performed to study the covariation between navicular shape and quantified locomotor data (SOM Table S2) in extant taxa. To do so, the function 'two.b.pls' from the package geomorph v. 4.0.3 (Adams and Otárola-Castillo, 2013) was used. This method uses 3D landmark data and performs a singular value decomposition, which decomposes the covariance matrix of the two blocks of variables into two matrices of eigenvectors (each one

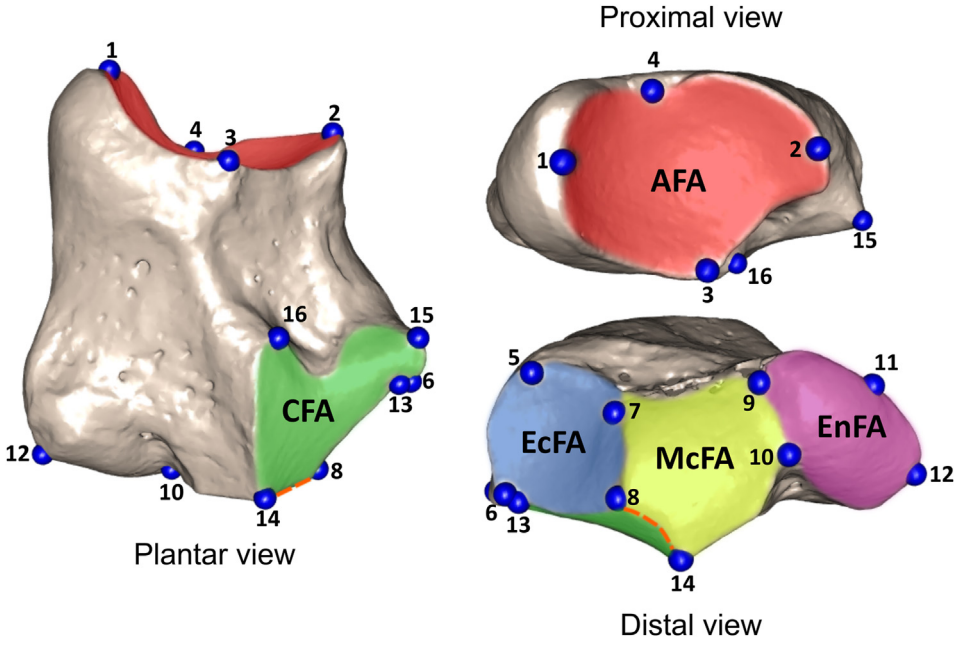

Figure 1. Landmark configuration and anatomy of the navicular bone. Plantar, proximal, and distal views of the navicular of *Eulemur fulvus* (USNM 542489, https://doi.org/10.17602/M2/M15828). McCuLength (mesocuneiform-cuboid contact length), depicting the contact between the McFA (mesocuneiform facet area) and CFA (cuboid facet area), is shown as an orange dotted line (between landmarks 8 and 14). Abbreviations: AFA = astragalar facet area; EnFA = entocuneiform facet area; EcFA = ectocuneiform facet area. See Table 1 for landmark definitions. (For interpretation of the references to color in this figure legend, the reader is referred to the Web version of this article.)

Table 1
Definition of the anatomical landmarks used in this study. To visualize placement of the landmarks on the navicular bone, see Figure 1.

Landmark	Definition
1	Most proximomedial point of the AFA
2	Most proximolateral point of the AFA
3	Plantarmost point of maximum curvature between LM1 and LM2
4	Dorsalmost point of maximum concavity between LM1 and LM2
5	Dorsolateralmost point of the EcFA
6	Plantarlateralmost point of the EcFA
7	Dorsalmost point of the contact between the EcFA and the McFA
8	Plantarmost point of the contact between the EcFA and the McFA
9	Dorsalmost point of the contact between the McFA and the EnFA
10	Plantarmost point of the contact between the McFA and the EnFA
11	Dorsomedialmost point of the EnFA
12	Plantarmedialmost point of the EnFA
13	Distolateralmost point of the CFA
14	Distomedialmost point of the CFA
15	Proximolateralmost point of the CFA
16	Proximomedialmost point of the CFA

Abbreviations: AFA = astragalar facet area; LM = landmark; EcFA = ectocuneiform facet area; McFA = mesocuneiform facet area; EnFA = entocuneiform facet area; CFA = cuboid facet area.

for one block of data) and a matrix of eigenvalues (the square-roots of eigenvectors; Rohlf and Corti, 2000; Bookstein et al., 2003). The significance of each linear combination is assessed by comparing the singular value to those obtained after resampling. If the partial least squares (PLS) covariation coefficient (r-PLS) is higher than the ones obtained from permutated blocks, its associated *p*-value is significant.

2.4. Reconstruction of early euprimate locomotor behavior

Prediction of the locomotor percentages To reconstruct the locomotor repertoire of early euprimates, we used the two sets of eigenvectors generated by the singular warp analysis performed on the previous covariance analysis (which was exclusively carried out on extant species). Similar approaches have previously been applied to reconstruct one block of shape variables from another block (e.g., Torres-Tamayo et al., 2020). We projected the species-means Procrustes shape coordinates belonging to the early euprimate species into the latent space generated after the singular warp analysis. We then used the coefficients obtained from the linear regression of the original latent variables to estimate the latent variables corresponding to the second block (derived from the quantified locomotor behavior data). The resulting variables can be projected back to obtain the quantified locomotor behavior of the early euprimate species. Finally, the locomotor percentages were predicted after reversing the arcsin square-root transformation and normalization (to ensure that their total sum was equal to 100).

To check the accuracy of this method, we performed a leave-one-out cross-validation (LOOCV) on the extant species set to predict their quantified locomotor behavior and compare it with their actual quantified locomotor behavior. We calculated the mean absolute error (MAE; Willmott and Matsuura, 2005) and plotted the estimated values against the original ones in a bivariate plot for each locomotor variable to compare them and assess if the predictive performance of this method varied depending on the estimated locomotor variable or the degree of locomotor specializations of some species (SOM Figs. S4 and S5; SOM Table S4).

Phylogenetic multivariate analysis of variance To assess the differences between navicular shape and foot type, taxonomic groups, and locomotor categories, we used a type II phylogenetic multivariate analysis of variance (MANOVA) with the function 'manova.gls' of the package mvMORPH v 1.1.6 (Clavel et al., 2015). The multivariate phylogenetic linear models were fitted with a Pagel's lambda by penalized likelihood using the 'mvgls' function of the package mvMORPH v1.1.6 (Clavel et al., 2015). In comparison to other modes, the advantage of using Pagel's lambda is that it provides more flexibility in estimating the error structure, as if we were fitting a phylogenetic mixed model while accounting for departure from Brownian motion (Clavel and Morlon, 2020). Significance was assessed using a Pillai statistic and 1000 permutations.

Phylogenetic discriminant function analysis To predict the locomotor category of fossil euprimates, we carried out a recently developed phylogenetic discriminant analysis. This consists of fitting a generalized least-squares model on the extant species data (training data set) to predict the locomotor category of each extinct euprimate species using both its Procrustes shape coordinates and its phylogenetic position. This new method is the first linear discriminant analysis which is both phylogeny-informed and applicable to high dimensional data sets (i.e., data sets containing more traits than individuals). The fitting of the model on the training data set was performed using the function 'mvgls.dfa' from the package mvMORPH v. 1.1.6 (Clavel et al., 2015), and the performance (misclassification rate) of the phylogenetic discriminant function analysis (pDFA) was assessed by performing a LOOCV on the training set. It consists of removing each individual one by one from the training set, performing the pDFA only on the remaining individuals, and checking if the locomotor category of the removed individual is well predicted. Then, we compared it to 1000 randomized predictions on the training set (SOM Fig. S6). Group membership to a locomotor class and posterior probabilities for fossil taxa were calculated using the function 'predict.mvgls.dfa' of the package mvMORPH v. 1.1.6 (Clavel et al., 2015). The predictions were made assuming an equal prior probability of belonging to the different locomotor categories since we do not have a priori knowledge of the prevalence of those categories in the geological period in which the extinct primates lived. Posterior probabilities are not necessarily a good estimate of the classification uncertainty because they may suffer from overfitting and do not accurately reflect out-of-sample prediction uncertainty (Qiao et al., 2009). As we previously did to evaluate the discriminant model performances, we assessed the classification uncertainty by using resampling techniques. For each fossil, we repeated the class prediction several times from models trained on different subsamples of the training set, and we computed the proportions in which the fossil was assigned to each locomotor class. Each training set was obtained using two different subsampling approaches inspired from leave-one-out and K-fold cross-validation. The leave-one-out subsampling approach consisted in removing one by one each extant individual from the training set and predicting the fossils' classes from a model trained on the remaining extant individuals. The K-fold subsampling approach consisted in randomly removing one-third of each locomotor class from the training set—since the smaller class contains three individuals—and predicting the fossils' classes from a model trained on the remaining extant individuals. The three-fold random subsampling was repeated 200 times. The K-fold approach tends to highlight more uncertainty in the predictions because it destabilizes more consequently the training set.

Convergence analyses To identify morphological convergence depending on similar locomotor behaviors, we utilized a phylogenetic ridge regression method of the package RRPhylo v. 2.5.8 (Castiglione et al., 2019). First, a phylogenetic ridge regression was performed on the tree with the species-means Procrustes shape

coordinates of the navicular, using the 'RRPhylo' function to obtain the branch-wise evolutionary rates and the ancestral character estimates at each node. After that, morphological convergence was tested using the function 'search.conv' of the package RRPhylo v. 2.5.8. Finally, the mean angle and the *p*-value of the mean angle were retrieved.

2.5. Navicular morphological evolution

Ancestral state reconstruction To assess the evolutionary model that best depicts the evolution of the first two principal components (PCs) of the PCA performed on the species-means Procrustes shape coordinates (Fig. 2), a maximum-likelihood approach was used with the functions 'mvBM,' 'mvOU,' 'mvEB,' and 'aicw' of the package mvMORPH v. 1.1.6 (Clavel et al., 2015). The ancestral morphotype for each node of the phylogenetic tree was estimated with the function 'estim' of the package mvMORPH v. 1.1.6 (Clavel et al., 2015). Finally, a phenogram plot, a projection of the phylogenetic tree in a space defined by a shape variable (y axis) and time (x axis), was performed using the function 'pheno' of the package phytools v. 0.7–20 (Revell, 2012) for each PC.

Rates of morphological evolution To test the morphological evolution of the navicular, we estimated the branch-specific evolutionary rates and rate shifts using the variable rates model applied in BayesTraits v. 3 (http://www.evolution.rdg.ac.uk/). The shifts in the rate of continuous trait evolution, which was modeled using a Brownian motion model, were detected with a reversible-jump Monte Carlo algorithm. The first 10 PCs of the phylogenetic PCA on the species-mean Procrustes shape coordinates, computed using the function 'phyl.pca' of the package phytools v. 0.7–20 (Revell, 2012) accounting for >99% of the overall variation in navicular shape, were used as an input. Ten independent chains were run for 200,000,000 iterations, sampling every 10,000 iterations, and the first 25,000,000 iterations were discarded as burn-in (SOM Table S5). Trace plots were examined, and the 10 independent chains that were stationary after burn-in were kept (SOM Fig. S7). The effective sample size (ESS) of the posterior samples (ESS < 100) as well as the convergence of the chains were assessed with a Gelman and Rubin's convergence diagnostic (SOM Tables S5 and S6), with the functions 'effectiveSize' and 'Gelman.diag' implemented in the package coda v. 0.19–4 (Plummer et al., 2005). Assessing the convergence of chains is critical to detect large deviations among the different chains (non-convergence) and ensure similar between-chain variances (Gelman and Rubin, 1992). The results were plotted on the tree using the function 'mytreebybranch' (https://github.com/anjgoswami/salamanders/blob/master/mytreerateplotter.R). Branch-specific average rates and the posterior probability of rate shifts (the mean of all ten independent chains) were summarized using the 'rjpp' and 'plotShift' functions of the package btrtools v. 0.0.0.9000 (https://github.com/hferg/btrtools/tree/master/R).

2.6. Shape visualization

To visualize shape differences in navicular shape between the extremes of the axes of the different analyses carried out, a thin-plate spline deformation of the 3D model of a navicular bone was carried out. Shape visualization of the effects of PCs, PLS, and discriminant function values was performed using the functions 'shape.predictor' and 'plotRefToTarget' of the package geomorph v. 4.0.3 (Adams and Otárola-Castillo, 2013) and 'shade3d' of the package rgl v. 0.100.47 (Adler and Murdoch, 2020). The specimen used as the reference was the navicular bone of *Eulemur fulvus* (USNM 542489), which is adequate to represent the mean shape of the sample.

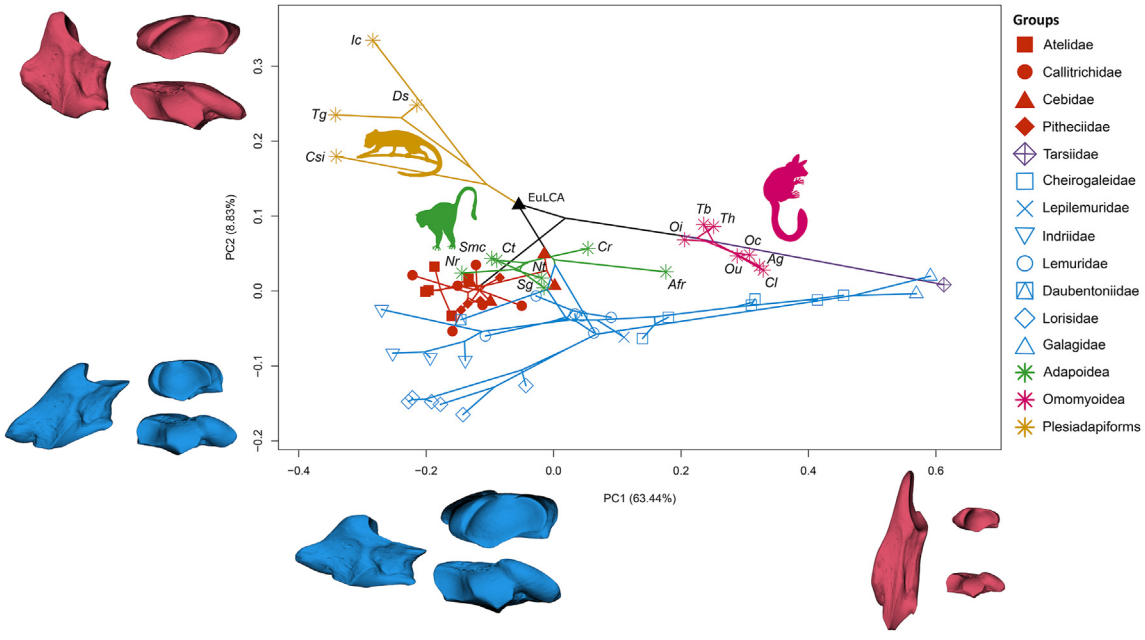

Figure 2. Phylomorphospace based on the first and second principal components (PCs of the principal component analysis carried out on the species-mean adjusted shape coordinates). Data points are color-coded by taxonomic group. The amount of variance explained by each PC is depicted below the axis in parenthesis. Navicular shapes associated with minimum (blue) and maximum (red) values along each PC (plantar, proximal, and distal views are shown from left to right and from top to bottom, as shown in Fig. 1). Thin plate splines correspond to the specimen of *Eulemur fulvus* USNM 542489. Abbreviations: EuLCA = euprimate last common ancestor; Th = *Tetonius homunculus*; Ag = *Arapahovius gazini*; Oi = Omomyidae indet.; Oc = *Omomys carteri*; Ou = *Ourayia uintensis*; Cl = *Chipetaia lamporea*; Tb = *Teilhardina brandti*; Afr = *Anchomomys frontanyensis*; Nr = *Notharctus robustior*; Nt = *Notharctus tenebrosus*; Ct = *Copelemur tutus*; Sg = *Smilodectes gracilis*; Smc = *Smilodectes mcgrewi*; Cr = *Cantius ralstoni*; Ic = *Ignacius clarforkensis*; Cs = *Carpolestes simpsoni*; Ds = *Dryomomys szalayi*; Tg = *Tinimomys graybulliensis*. (For interpretation of the references to color in this figure legend, the reader is referred to the Web version of this article.)

3. Results

3.1. Navicular shape variation among primates

No significant correlation is found between navicular shape and $\log_{10}$-transformed centroid size in the entire sample (Pillai's trace = 0.470, $p = 0.756$) or among euprimates alone (Pillai's trace = 0.561, $p = 0.415$). Although navicular centroid size and body mass are significantly correlated ($r^2 = 0.299$, $p < 0.001$; see SOM Fig. S2), three species of vertical clingers and leapers (*T. spectrum*, *G. moholi*, and *S. alleni*) are clear outliers of the linear regression, displaying larger navicular centroid sizes than expected given their body masses. Thus, we repeated the allometric analysis on euprimates excluding these three species and found a significant correlation between navicular shape and $\log_{10}$-transformed centroid size, indicating intrinsic allometric effects (smaller naviculars are relatively proximodistally longer compared to larger ones) in most euprimates (Pillai's trace = 0.594, $p = 0.031$).

The phylomorphospace of the first two PCs of a PCA based on the species-mean Procrustes shape coordinates differentiates species by locomotor behavior and foot type (Fig. 2). PC 1 (63.44% of the total variance) separates species depending on the degree of proximodistal elongation of the navicular, hence denoting a much wider distribution in tarsi-fulcrumating species (comprising extant strepsirrhines, tarsiers, and the extinct adapiforms and omomyiforms) than in metatarsi-fulcrumating ones (extant platyrrhines and plesiadapiforms). Slow climbers (SC, lorisids), large vertical clingers and leapers (LVCL, indriids), suspensors/clamberers (SUS/CLA, atelids), clawed-leapers (CL, callitrichids), and many arboreal quadrupeds/large leapers (AQ/LL, cebids, pitheciids, and *Daubentonia madagascariensis*) display negative scores with a proximodistally short navicular. In contrast, the small-sized vertical clingers and leapers (tarsiids and galagids), which possess a very proximodistally elongated navicular, display positive scores. Species with a moderate proximodistal elongation, such as the cheirogaleids, the lemurids, and the large VCL *Lepilemur mustelinus*, display intermediate scores. Extinct species are distributed along the first axis, forming three differentiated clusters: omomyiforms overlap with cheirogaleids, displaying moderate proximodistal elongation without reaching the extreme shown by tarsiids and galagids; adapiforms occupy the same range as lemurids and *L. mustelinus*; and plesiadapiforms fall apart of the other species, exhibiting a proximodistally short navicular outside the euprimate morphospace.

Principal component 2 (8.83% of the total variance) reflects changes in the shape of the astragalar facet as well as the arrangement of the cuneiform facets. Plesiadapiforms differ from the other species in displaying a more transversely elongated astragalar facet on the medial side and having a medially and plantarly extended entocuneiform facet. In contrast, all euprimates display an ovoid astragalar facet and more aligned cuneiform facets, though some small leapers like tarsiers possess a small and plantarly compressed mesocuneiform facet, and others, such as several anthropoids, display an L-shaped arrangement of the facets.

3.2. Navicular shape as a proxy for locomotion

Phylogenetic MANOVA results indicate that among living euprimate species, there are significant shape differences between locomotor categories (Pillai's trace = 3.732, $p = 0.003$) and foot type (Pillai's trace = 1.246, $p = 0.046$), thus indicating that both locomotor behavior and type of foot posture impact navicular shape.

The first two blocks of the 2B-PLS analysis for the entire extant sample (Fig. 3A) show significant covariation between navicular shape and locomotion (r-PLS = 0.435, $p = 0.041$). Proximodistally elongated naviculars with a more proximally projecting medial side at the astragalar facet are correlated with leaping, whereas proximodistally short and mediolaterally wide naviculars are associated with preference for scrambling and clambering, bridging, and quadrupedal behaviors. However, among large VCL species, indriids (indicated in the figure) depart from the general trend and display proximodistally shortened naviculars despite their proclivity for leaping, thus indicating that proximodistal elongation is indicative of leaping behavior in tarsi-fulcrumating species but not in tarsi-rotator ones. Because of the importance of taking the type of foot posture into account, we repeated the analysis, including only the tarsi-fulcrumating species. When tarsi-fulcrumators are considered alone (Fig. 3B), a stronger correlation is found between navicular shape and locomotion. Again, proximodistal elongation of the navicular is related to leaping proclivity, whereas a proximodistally short and mediolaterally broader navicular is characteristic of more suspensory, bridging, and quadrupedal animals (r-PLS = 0.824, $p < 0.001$).

3.3. Reconstruction of the locomotor repertoire of early primates

The estimated locomotor percentages (Fig. 3A, B; Table 2) for early euprimate species depict two main patterns of locomotor repertoires. Omomyiforms as well as *A. frontanyensis* are characterized by intermediate to high reliance on leaping (34–65%), moderate degrees of quadrupedalism and climbing (13–32%), and more modest values for the other locomotor variables (<10%, most of them <5%). Among extant species, the locomotor repertoires of *Microcebus* and *Mirza* are the ones that more closely resemble the reconstructed ones for these taxa. Except for *A. frontanyensis*, the other adapiforms display higher percentages of quadrupedalism (30–50%) and climbing (21–40%) and variable reliance on leaping (7–33%), although always below the percentages displayed by omomyiforms. Some species, like *Notharctus robustior*, also display moderate percentages of suspension (17%), whereas bridging and scrambling/clambering percentages are very low for all species (less than 6%). These species are reconstructed as above-branch quadrupeds and climbers, and the better analogues for their locomotor repertoire are the lemurids, especially the larger forms such as *Lemur catta* or *Varecia variegata*. There are no important differences between the predictions obtained from the analysis carried out on the entire extant sample and the sample comprised only by tarsi-fulcrumators, although the latter are slightly less scattered across the fossil sample (omomyiforms and *A. frontanyensis* on the one hand, and the other adapiforms on the other, show more consistent within-group percentages) and yielded smaller MAEs for all locomotor variables (SOM Table S4).

The phylogenetically informed discriminant analysis has a misclassification rate of 0.152 after performing a LOOCV on the training set (extant ones). Two estimates of group membership classification confidence for each extinct species (comparing two subsampling techniques: leave-one-out and K-fold cross-validation) are presented in Table 3. Figure 4 is the graphical result of the pDFA (the plot of the species on the principal discriminant axes, which are those that better discriminate among the different locomotor categories). Omomyiforms are classified as cheirogaleid generalists (*Omomys carteri*, *Ourayia uintensis*, *Chipetaia lamporea*, and Omomyidae indet.), arboreal quadrupeds/large leapers (*Tetonius homunculus*), or small VCL (*Teilhardina brandti* and *Arapahovius gazini*). Conversely, all adapiforms fall into the arboreal quadrupeds/large leapers category except for *A. frontanyensis*, which is classified as a large VCL.

Convergence analyses (Table 4) confirmed the similarities between adapiforms and extant arboreal quadrupeds/large leapers

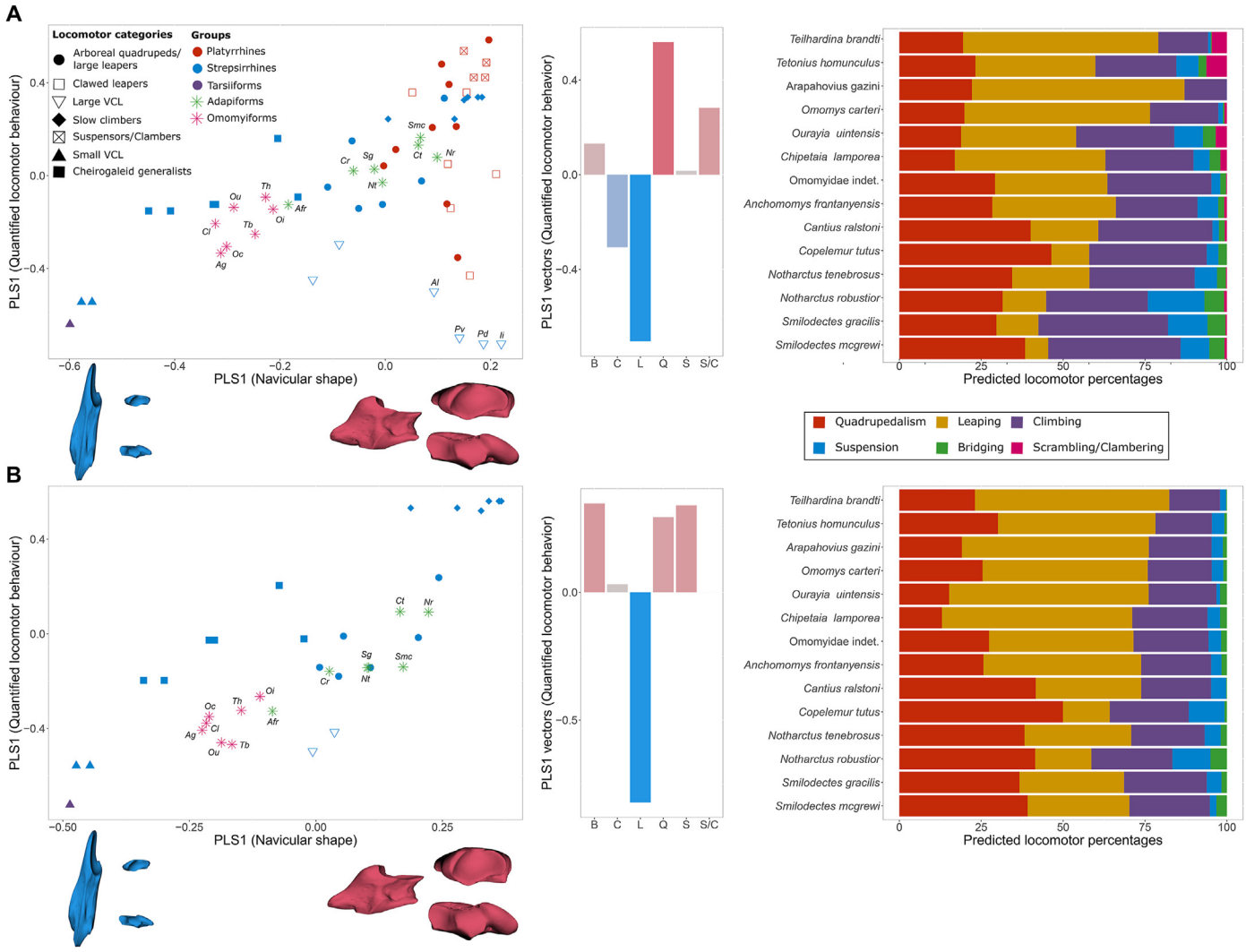

Figure 3. Results of the two-block partial least squares (2B-PLS) between the species-mean Procrustes shape coordinates and quantified locomotor data for all extant species included in this study (A) and tarsi-fulcrumating ones (B). Data points are color coded by taxonomic group and shape is coded by locomotor category. The vectors of the first PLS axis of the locomotor variables are plotted in the right side of the figure. The predicted locomotor percentages for the fossil species are presented in a bar chart located next to the vectors for the first PLS axis for each condition. Navicular shapes associated with minimum (blue) and maximum (red) values of covariation are plotted below each scatterplot (plantar, proximal, and distal views are shown, from left to right and from top to bottom, as shown in Fig. 1). Thin plate splines correspond to the specimen of *Eulemur fulvus* USNM 542489. Abbreviations: Q = quadrupedalism; B = bridging; C = climbing; L = leaping; S = suspension; S/C = scrambling/clambering; Th = *Tetonius homunculus*; Ag = *Arapahovius gazini*; Oi = Omomyidae indet.; Oc = *Omomys carteri*; Ou = *Ourayia uintensis*; Cl = *Chipetaia lamporea*; Tb = *Teilhardina brandti*; Afr = *Anchomomys frontanyensis*; Nr = *Notharctus robustior*; Nt = *Notharctus tenebrosus*; Ct = *Copelemur tutus*; Sg = *Smilodectes gracilis*; Smc = *Smilodectes mcgrewi*; Cr = *Cantius ralstoni*; Al = *Avahi laniger*; Ii = *Indri indri*; Pd = *Propithecus diadema*; Pv = *Propithecus verreauxi*. (For interpretation of the references to color in this figure legend, the reader is referred to the Web version of this article.)

and indicated a greater degree of convergence with lemurids than with platyrrhines. In contrast, no convergence was found between adapiforms (excluding *A. frontanyensis*) and cheirogaleids. Among adapiforms, the middle Eocene notharctid genera (*Smilodectes* and *Notharctus*) also presented significant convergence with the group of specialized large VCL (indriids, *Hapalemur griseus*, and *L. mustelinus*). Conversely, *A. frontanyensis* is classified as a large VCL in the previous pDFA but shows no convergence with this group. Omomyiforms show convergence with the small VCL (*T. spectrum* and the galagids), with the cheirogaleids, and with *A. frontanyensis*. No convergence was found between omomyiforms and either the extant arboreal quadrupeds/large leapers or the adapiforms excluding *A. frontanyensis*. Lastly, no convergence was found between the plesiadapiforms and the callitrichids (clawed leapers) and the lorisids (slow climbers).

3.4. Navicular evolution across the archaic primate–euprimate transition

An 'Early Burst' model is the one that best explains the evolution of PC1, showing a diversification of the proximodistal elongation of the navicular early in euprimate evolutionary history (Fig. 5A; Table 5). By contrast, PC2 evolution is best described by an 'Ornstein–Uhlenbeck' model, depicting stabilizing selection toward an euprimate-like navicular, with more ovoid astragalar facet and straighter arrangement of the cuneiform facets (Fig. 5B; Table 5). Important shifts in rates of navicular evolution occur early in primate evolution (Fig. 6; SOM Fig. S7). Remarkably, mean evolutionary rates are extremely high in the branch leading to the euprimate ancestor. Other significant shifts occur earlier, during the radiation of plesiadapiforms, and across the clade composed of the

Table 2
Predicted locomotor repertoire for each extinct euprimate species. Locomotor percentages were calculated after normalization and reversion of the arcsin square root transformation on the estimated quantified locomotor behavior (see Materials and methods).

Species	Q		L		C		S		B		S/C	
	Entire sample	Tf	Entire sample	Tf	Entire sample	Tf	Entire sample	Tf	Entire sample	Tf	Entire sample	Tf
Tetonius homunculus	23.221	30.124	36.652	48.074	24.660	17.220	6.793	3.765	2.359	0.816	6.315	0.000
Arapahovius gazini	22.171	19.091	64.924	57.098	12.728	19.130	0.077	3.464	0.009	1.217	0.091	0.000
Omomyidae indet.	29.220	27.367	34.317	44.136	31.738	22.899	2.723	3.829	1.714	1.769	0.289	0.000
Omomys carteri	19.860	25.412	56.697	50.419	20.832	19.552	1.401	3.537	0.434	1.080	0.776	0.000
Ourayia uintensis	18.866	15.187	35.114	60.949	29.972	20.677	8.752	1.133	3.850	2.046	3.447	0.008
Chipetaia lamporea	16.930	13.006	45.972	58.101	26.900	22.981	4.923	3.858	3.283	2.053	1.992	0.001
Teilhardina brandti	19.444	23.082	59.632	59.353	15.167	15.456	0.792	1.823	0.314	0.285	4.651	0.000
Anchomomys frontanyensis	28.382	25.683	37.752	48.149	24.857	21.311	6.372	3.192	1.796	1.660	0.842	0.004
Notharctus robustior	31.520	41.483	13.308	17.143	31.011	24.745	17.279	11.622	6.010	5.003	0.872	0.003
Notharctus tenebrosus	34.429	38.204	23.614	32.606	32.127	22.408	6.809	4.899	2.699	1.880	0.323	0.003
Copelemur tutus	46.422	49.954	11.553	14.285	35.858	24.122	3.597	10.889	2.554	0.747	0.016	0.004
Smilodectes gracilis	29.627	36.695	12.842	31.928	39.545	25.238	12.076	4.470	5.456	1.665	0.455	0.004
Smilodectes mcgrewi	38.388	39.151	7.067	31.088	40.396	24.539	8.793	2.028	4.595	3.181	0.761	0.014
Cantius ralstoni	40.079	41.644	20.684	32.194	34.811	21.307	1.979	4.621	1.774	0.233	0.673	0.001

Abbreviations: Tf = tarsi-fulcrumators; Q = quadrupedalism; L = leaping; C = climbing; S = suspension; B = bridging; S/C = scrambling/clambering.

Table 3
Results of the phylogenetic discriminant analysis. Locomotor category predicted for each species and two estimates of group membership classification confidence (LOOCV and K-fold) are provided.[a]

Species	Classification	AQ/LL		CG		CL		LVCL		SC		SVCL		SUS/CLA	
		LOOCV	K-fold	LOOCV	K-fold	LOOCV	K-fold	LOOCV	K-fold	LOOCV	K-fold	LOOCV	K-fold	LOOCV	K-fold
Tetonius homunculus	AQ/LL	**0.891**	0.447	0.109	**0.478**	0.000	0.000	0.000	0.000	0.000	0.000	0.000	0.075	0.000	0.000
Arapahovius gazini	SVCL	0.000	0.000	0.022	0.433	0.000	0.000	0.000	0.000	0.000	0.000	**0.978**	**0.567**	0.000	0.000
Omomyidae indet.	CG	0.022	0.190	**0.978**	**0.752**	0.000	0.000	0.000	0.007	0.000	0.000	0.000	0.052	0.000	0.000
Omomys carteri	CG	0.000	0.000	**0.978**	**0.842**	0.000	0.000	0.000	0.000	0.000	0.000	0.022	0.158	0.000	0.000
Ourayia uintensis	CG	0.000	0.000	**0.978**	**0.877**	0.000	0.000	0.000	0.000	0.000	0.000	0.022	0.123	0.000	0.000
Chipetaia lamporea	CG	0.000	0.000	**0.870**	0.395	0.000	0.000	0.000	0.000	0.000	0.000	0.130	**0.605**	0.000	0.000
Teilhardina brandti	SVCL	0.000	0.107	0.435	**0.563**	0.000	0.000	0.000	0.010	0.000	0.000	**0.565**	0.320	0.000	0.000
Anchomomys frontanyensis	LVCL	0.065	0.357	0.000	0.222	0.000	0.000	**0.935**	**0.422**	0.000	0.000	0.000	0.000	0.000	0.000
Notharctus robustior	AQ/LL	**0.978**	**0.702**	0.000	0.000	0.000	0.007	0.022	0.278	0.000	0.000	0.000	0.000	0.000	0.013
Notharctus tenebrosus	AQ/LL	**1.000**	**0.988**	0.000	0.000	0.000	0.000	0.000	0.012	0.000	0.000	0.000	0.000	0.000	0.000
Copelemur tutus	AQ/LL	**1.000**	**0.982**	0.000	0.000	0.000	0.018	0.000	0.000	0.000	0.000	0.000	0.000	0.000	0.000
Smilodectes gracilis	AQ/LL	**1.000**	**0.875**	0.000	0.000	0.000	0.000	0.000	0.125	0.000	0.000	0.000	0.000	0.000	0.000
Smilodectes mcgrewi	AQ/LL	**1.000**	**0.985**	0.000	0.000	0.000	0.008	0.000	0.007	0.000	0.000	0.000	0.000	0.000	0.000
Cantius ralstoni	AQ/LL	**1.000**	**0.995**	0.000	0.000	0.000	0.000	0.000	0.005	0.000	0.000	0.000	0.000	0.000	0.000

Abbreviations: LOOCV = leave-one-out cross-validation; K-fold = K-fold cross-validation; AQ/LL = arboreal quadrupeds/large leapers; CG = cheirogaleid generalists; CL = clawed leapers; LVCL = large vertical clingers and leapers; SC = slow climbers; SVCL = small vertical clingers and leapers; SUS/CLA = suspensors/clamberers.
[a] The highest estimate for each method is marked in bold.

early to middle Eocene notharctid species and within groups characterized by a particular locomotor behavior, such as the indriids, the lorisids, and the atelids.

4. Discussion

The study of early euprimate locomotor diversity is essential to understand the factors that led to their origin and early diversification. A substantial reorganization of the postcranial skeleton, including the tarsus, has been observed during the archaic primate–euprimate transition (Dagosto, 1988, 2007). Our study provides new clues on such a transition, shedding light on the remarkably diverse locomotor behavior of early euprimates on the basis of navicular shape, which emerges as a reliable proxy for primate locomotor behavior.

4.1. Understanding variation in navicular shape among primates

The elongation of different tarsal elements, such as the talar neck, the cuboid, the navicular, or the distal part of the calcaneus, is informative about the locomotor behavior of extinct taxa (Decker and Szalay, 1974; Gebo, 1988; Dagosto, 1988, 2007; Moyà-Solà et al., 2012; Boyer et al., 2013). However, the functional association between tarsal elongation and leaping does not hold for some groups, such as indriids, which are highly committed leapers despite possessing a proximodistally short navicular (Gebo and Dagosto, 1988). Other taxa, such as lemurids and anthropoids, display a wide variation in leaping frequency among taxa with similar navicular shape, thus hampering locomotor inferences solely on this basis (Crompton et al., 1987; Gebo, 1987a; Oxnard et al., 1990). Biomechanical studies of leaping have shown there are various constraints related to the size of the animal (Demes and Günther, 1989; Demes et al., 1996, 1999), leading to different anatomical solutions (Alfaro et al., 2005; Wainwright et al., 2005). Small-bodied leapers like tarsiers or small galagids must accelerate over small distances and hence need to maximize the time and distance required to generate enough impulse during takeoff. For this reason, small leapers possess very elongated feet, including the navicular in the midtarsal region (Hall-Crags, 1965; Demes and Günther, 1989). In contrast, large VCL species are constrained by the more limited force available to accelerate (muscle force increases as a function of area, whereas weight increases as a function

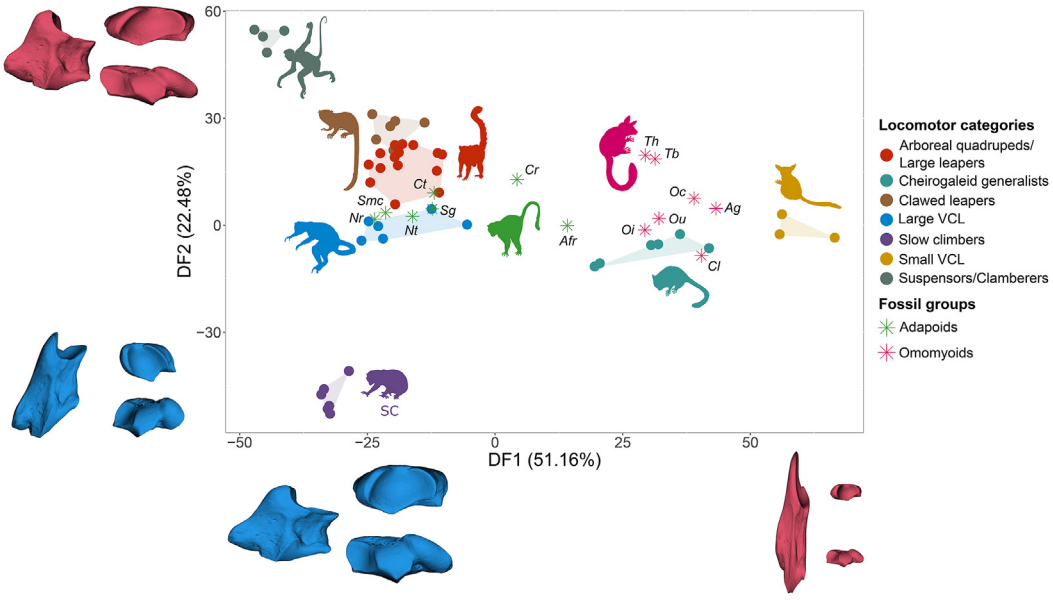

Figure 4. Phylogenetic discriminant analysis based on the species mean-adjusted shape coordinates and locomotor categories. Data points are color coded by locomotor category (extant species) or taxonomic group (extinct species). Navicular shapes associated with minimum (blue) and maximum (red) values of each discriminant function (DF; plantar, proximal, and distal views are shown, from left to right and from top to bottom, as shown in Fig. 1). Thin plate splines correspond to the specimen of *Eulemur fulvus* USNM 542489. Abbreviations: Th = *Tetonius homunculus*; Ag = *Arapahovius gazini*; Oi = Omomyidae indet.; Oc = *Omomys carteri*; Ou = *Ourayia uintensis*; Cl = *Chipetaia lamporea*; Tb = *Teilhardina brandti*; Afr = *Anchomomys frontanyensis*; Nr = *Notharctus robustior*; Nt = *Notharctus tenebrosus*; Ct = *Copelemur tutus*; Sg = *Smilodectes gracilis*; Smc = *Smilodectes mcgrewi*; Cr = *Cantius ralstoni*. (For interpretation of the references to color in this figure legend, the reader is referred to the Web version of this article.)

Table 4
Results of the convergence analyses performed on species-mean adjusted shape coordinates between extinct and living primate species.[a]

Comparison	Mean angle	*p*-value
Adapiforms and arboreal quadrupeds/ large leapers	13.332	**0.001**
Adapiforms and arboreal quadrupeds/ large leapers (Lemuridae)	9.494	**0.009**
Adapiforms and arboreal quadrupeds/ large leapers (Cebidae and Pitheciidae)	12.396	**0.049**
Adapiforms and cheirogaleid generalists	15.643	0.162
Middle Eocene notharctids (*Smilodectes* and *Notharctus*) and large vertical clingers and leapers	8.532	**0.002**
Anchomomys frontanyensis and large vertical clingers and leapers	18.470	**0.32**
Omomyiforms and small vertical clingers and leapers	11.429	**0.011**
Omomyiforms and cheirogaleid generalists	9.103	**0.006**
Omomyiforms and arboreal quadrupeds/large leapers	15.683	0.172
Omomyiforms and North American notharctids (*Cantius*, *Copelemur*, *Smilodectes* and *Notharctus*)	15.475	0.162
Omomyiforms and *Anchomomys frontanyensis*	8.330	**0.002**
Plesiadapiforms and clawed leapers	20.396	0.518
Plesiadapiforms and small climbers	22.371	0.687

[a] Significant results are indicated in bold for $p < 0.05$.

of volume) and hence do not show such an elongation of the tarsal elements (Gebo and Dagosto, 1988; Demes and Günther, 1989; Demes et al., 1996).

Foot-type posture also impacts the degree of proximodistal elongation of the navicular. Tarsi-fulcrumating species display a broader range of navicular elongation, as shown by their distribution along PC1 of the phylomorphospace (Fig. 2), and significant shape differences are found between groups. This distinction is linked to the loss of available load arm, that tarsi-fulcrumators compensate for by means of a greater elongation of the tarsal region (Morton, 1924; Moyà-Solà et al., 2012).

Covariation analyses confirm the relationship between navicular shape and locomotor behavior, as well as the importance of considering foot-type posture. Both 2B-PLS analyses (Fig. 3) relate proximodistal elongation of the navicular with leaping proclivity, whereas proximodistally short naviculars are associated with quadrupedalism, bridging, and scrambling and clambering (Gebo, 1988). However, proximodistal elongation is only correlated with locomotor behavior among tarsi-fulcrumating species (Fig. 3B). For example, indriids display a very proximodistally short navicular despite their high proclivity toward leaping, with broad and shallow astragalar and cuneiform facets, as well as a more sellar-shaped cuboid facet, features more related to climbing rather than leaping behavior (Gebo and Dagosto, 1988). This set of features is likely related to their particular foot type, in which the foot does not act as a propulsor but as a force transducer (Demes et al., 1996). Among metatarsi-fulcrumators, suspensors, scramblers, and clamberers also display broader naviculars with wide and shallow astragalar and cuneiform facets, whereas more quadrupedal and leaping species possess narrow naviculars with deeper facets that enhance the stability of the astragalonavicular joint (Decker and Szalay, 1974). Cuneiform facets (in particular the entocuneiform facet) are also broader and shallower in more suspensory or climbing primates like lorisids (Gebo, 1989), compared to the narrower and more protuberant facets displayed by more quadrupedal or leaping species, such as galagids, in which the arrangement and shape of the facets limit rotational movements (Hall-Craggs, 1966; Gebo, 1987b). Tarsiers are an exception to this trend, as they possess a navicular capable of rotating in both its proximal and distal ends to achieve foot inversion (Gebo, 1987b). Differences in the shape of the cuboid facet also exist between saltatory or more suspensory species as well as climbing taxa, the latter presenting broader and

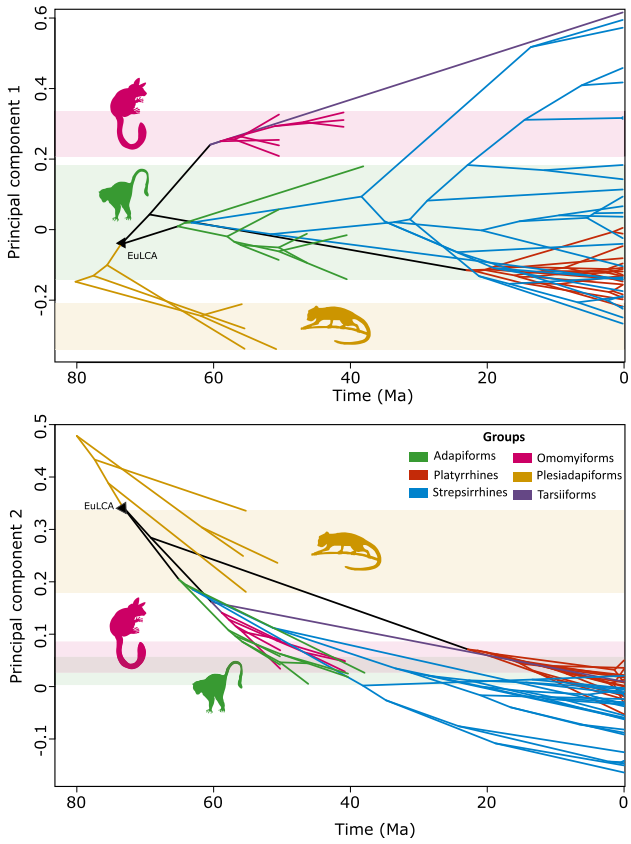

Figure 5. Phenogram based on the (A) first and (B) second principal components (Fig. 2) for all extant and fossil species and the reconstructed internal nodes following an 'Early Burst' (A) or an 'Ornstein-Uhlenbeck' (B) evolutionary model (see also Table 5). Tree branches are color-coded by taxonomic group. The euprimate last common ancestor is indicated by a black triangle in its corresponding node. Adapiform, omomyiform, and plesiadapiform ranges and their overlap with the other groups are indicated by blue, green, and yellow shades, respectively. (For interpretation of the references to color in this figure legend, the reader is referred to the Web version of this article.)

Table 5
Results of the evolutionary model comparison for the first and second principal components (PC) of the principal component analysis performed on the species-mean adjusted shape coordinates. The highest AICw for each PC is in bold.

Axis	Evolutionary model	Loglikelihood	AIC	AICw
PC1	BM	47.210	−90.224	0.026
	OU	47.867	−87.056	0.007
	EB	**51.849**	**−97.297**	**0.968**
PC2	BM	103.954	−203.712	0.001
	OU	**113.198**	**−217.718**	**0.996**
	EB	106.559	−206.718	0.004

Abbreviations: AICc = Akaike Information Criterion corrected; AICw = weighted AIC; BM = Brownian motion; OU = Ornstein-Uhlenbeck; EB = Early Burst.

mediolaterally extended cuboid facets. This last feature is also relevant from a phylogenetic viewpoint, as the contact between the cuboid and mesocuneiform facets is a strepsirrhine synapomorphy that has been related to increased midtarsal folding of the foot, an adaptation toward the use of vertical supports (Beard et al., 1988; Dagosto, 1988).

4.2. The diverse locomotion of early euprimates

Among early euprimates, omomyiforms have been described as agile climbing and running animals, with active arboreal locomotion and high proclivity for leaping (Gebo, 1988; Anemone and Covert, 2000; Rose et al., 2011; Gebo et al., 2012, 2015; Boyer et al., 2013). This is revealed in the phylomorphospace (Fig. 2), in which omomyiforms display relatively similar scores to some extant small-bodied leapers (such as *Microcebus* or *Mirza*), although they do not overlap with any extant species and do not reach the extreme values displayed by specialized small VCL forms like *T. spectrum* or the galagids, suggesting that they lacked a specialized VCL locomotion. Moreover, the results from the prediction of their locomotor repertoire (Fig. 3; Table 2) indicate a moderate to high proclivity for leaping, combined with lower percentages of quadrupedalism and climbing. Phylogenetic discriminant analysis classifies omomyiform species either as cheirogaleid generalists (*C. lamporea*, *O. uintensis*, *Omomys carteri*, and Omomyidae indet. [UCMP V 134984]) or small VCL (*T. brandti* and *A. gazini*), apart from *T. homunculus*, which falls in the arboreal quadrupeds/large leapers category (Table 3). The scatterplot of the discriminant analysis (Fig. 4) and the results of the convergence analyses (Table 4) illustrate overall similarities between omomyiforms and both small VCL species and cheirogaleid generalists, indicating an active (yet not specialized for VCL) locomotor behavior for these species (Gebo, 1988). Interestingly, when the robustness of each classification is assessed by means of a subsampling technique (LOOCV and K-fold cross-validation), we find that the locomotor category that better suits to all omomyiforms is cheirogaleid generalists, whereas some specimens (belonging to *T. homunculus* and Omomyidae indet.) show moderate propensity for the arboreal quadrupeds/large leapers category, and others (including *A. gazini*, *T. brandti*, or *C. lamporea*) are more frequently classified as small VCL. The relatively elongated navicular of omomyiforms, which falls within the cheirogaleid range, is the most important feature related with increased leaping behavior (Gebo, 1988; Boyer et al., 2013). In addition, the proximal protrusion of the proximomedial side of the astragalar facet and the shallower and reduced cuneiform facets without a contact between the mesocuneiform and the cuboid facets likely limit the degree in which rotational movements were accomplished along these articulations (Dagosto, 1988; Marigó et al., 2020). The smaller estimated body size for most omomyiforms is also an important feature that has been related to a more agile locomotor repertoire (Rose, 1994). However, larger-sized omomyiforms such as *O. uintensis* and *C. lamporea* are still classified in our analyses as relatively agile unspecialized leapers. This agrees with previous studies (Dunn et al., 2006; Dunn, 2010) and indicates that an increased leaping behavior was a shared feature within the omomyiform locomotor repertoire. *Tetonius homunculus*, which compared to other omomyiforms shows in our analyses more propensity for quadrupedal and climbing locomotion, is also the one displaying less navicular proximodistal elongation, in accordance with other features in the calcaneus and the astragalus, such a slightly shorter distal calcaneus and a mediolaterally broader astragalar head (Gebo, 1988). One omomyiform genus, *Necrolemur*, for which the navicular is unknown, displays similar tarsier-like morphological specialization in its hindlimbs, and likely had a different locomotor repertoire than the species present in our study. This would add more locomotor diversity to this group, which likely included from active arboreal quadrupeds to specialized VCL in the case of some later forms (Dagosto, 1985; Gebo, 1987b).

Adapiforms are considered basal strepsirrhines by most cladistic analyses (Seiffert et al., 2005; Williams et al., 2010). Moreover, adapiforms share derived pedal traits with extant strepsirrhines, whereas omomyiforms usually retain a more primitive condition (Decker and Szalay, 1974; Gebo, 1986, 1988; Dagosto, 1988, 2007). Adapiforms are generally larger than omomyiforms and characterized by less elongated tarsal bones, indicating that they were predominantly above branch arboreal quadrupeds with less proclivity for leaping (Rose and Walker, 1985; Covert, 1988; Gebo,

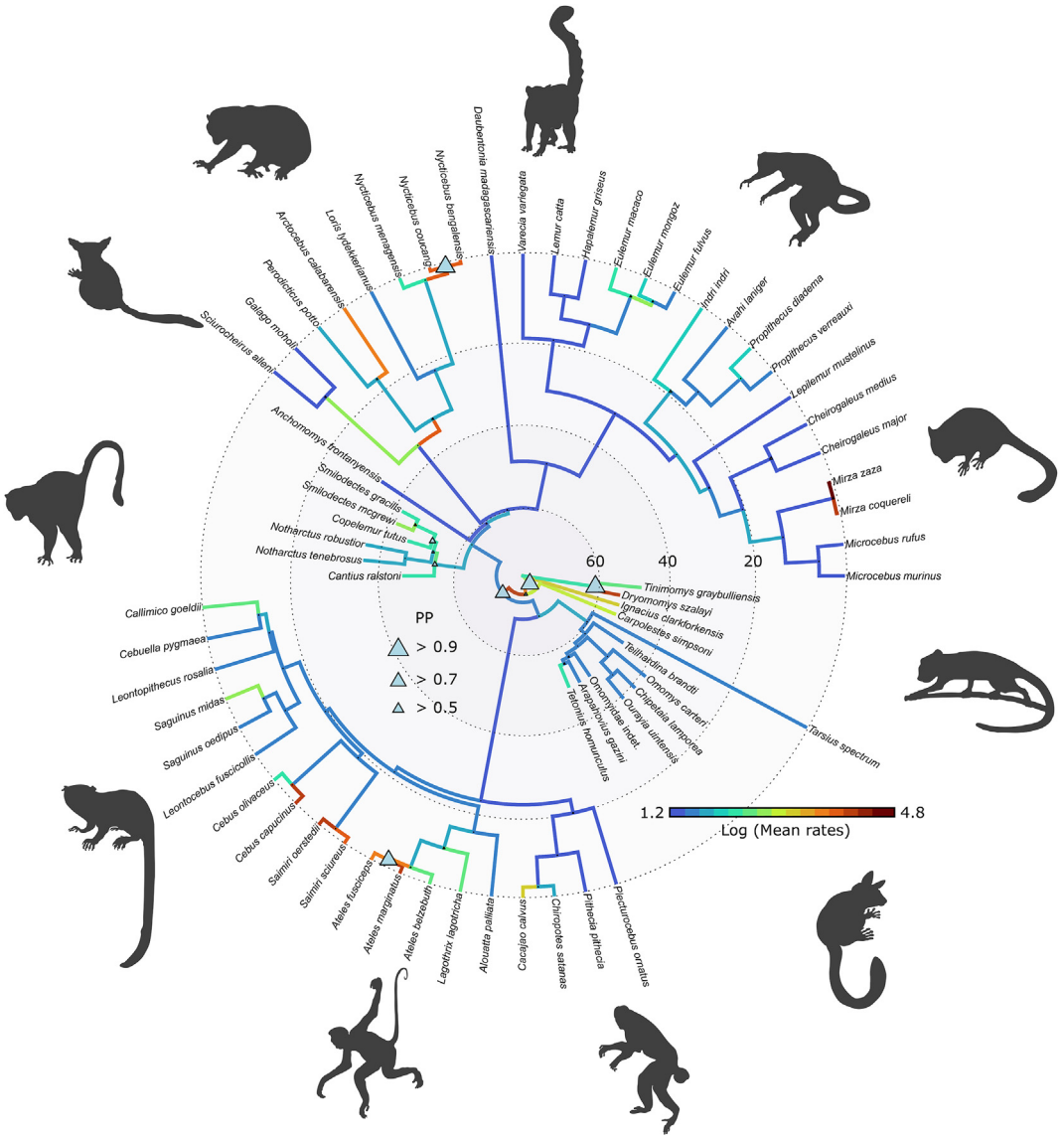

Figure 6. Evolutionary rates and rate shifts for navicular shape in extant and extinct primates. Branch rates are color-coded (warmer colors indicate faster evolutionary rates while cooler colors represent slower evolutionary rates). High probability shifts in evolutionary rates are indicated by blue triangles. The relative size of the triangles represents the posterior probabilities (PP) of the rate shifts (see SOM Fig. S7 to visualize the PP of rate shifts). (For interpretation of the references to color in this figure legend, the reader is referred to the Web version of this article.)

1988; Gebo et al., 1991; Boyer et al., 2013), as supported by our results (Figs. 3–5; Tables 2–4). The only exception is the small-bodied adapiform *A. frontanyensis*, which possesses an omomyiform-like tarsal elongation (Marigó et al., 2016, 2020). This is indicated in the phylomorphospace (Fig. 2), in which *A. frontanyensis* falls very close to the omomyiform cluster. Despite these morphological similarities, there is no doubt that *A. frontanyensis* is a basal strepsirrhine instead of an omomyiform. Apart from the dental characters that identify *A. frontanyensis* as a strepsirrhine (Marigó et al., 2011), its navicular displays an unambiguous strepsirrhine synapomorphy: a contact between the mesocuneiform and the cuboid facets (Dagosto, 1988). Interestingly, the contact between these facets in *A. frontanyensis* is more restricted than in most extant strepsirrhines, probably a primitive retention from the ancestral euprimate, given that *Cantius ralstoni*, the most basal adapiform of our sample, also displays a very short contact (Beard et al., 1988; Marigó et al., 2020). The prediction of its locomotor repertoire, similar to that of some omomyiform species (Fig. 3; Table 2), and the results from the convergence analyses (Table 4) also highlight the similarities in navicular shape between *A. frontanyensis* and omomyiforms. Nevertheless, the more bulbous cuneiform facets and the contact between the mesocuneiform and cuboid facets in *A. frontanyensis* are likely related to a more inverted foot posture than in omomyiforms, which some authors have interpreted as an adaptation for the small branch niche (Marigó et al., 2020). Considering this, an active arboreal locomotion for *A. frontanyensis*, similar to that of *Cheirogaleus* or *Mirza*, is the best interpretation for its locomotor behavior. Interestingly, convergence analyses also yielded significant convergence between adapiforms and extant large VCL species. This is at odds with our prediction of the notharctid locomotor repertoire, which is dominated by quadrupedalism and climbing (Table 4), and thus is closer to that of above-branch quadrupeds than specialized VCL. In addition, some authors have noted that the foot of notharctids lacked some morphological adaptations required to engage in VCL locomotion, such as a derived adductor grasping mode (sensu

Gebo, 1985; Gebo and Dagosto, 1988), thus strengthening our view that these animals were more likely non-specialized arboreal quadrupeds, like the ringtail (*Lemur catta*) and ruffed lemurs (*V. variegata*). Similarly, the phylogenetic discriminant analysis classifies *A. frontanyensis* as a large VCL, in disagreement with the results of other analyses for this taxon. We hypothesize that some similarities in navicular shape and elongation between *A. frontanyensis* and the non-indriid large VCL (*H. griseus* and *L. mustelinus*) might have led to this result. In addition, when resampling techniques (LOOCV and K-fold CV) are performed to assess the classification uncertainty of the pDFA, *A. frontanyensis* shows moderate propensity for the AQ/LL and CG categories, thus indicating a more agile arboreal locomotor behavior.

4.3. The archaic primate–euprimate transition

Our results support that early euprimates underwent a rapid adaptive diversification very early in their evolutionary history, which allowed them to occupy different arboreal niches (Figs. 5 and 6; Table 5). The postcranial remains of plesiadapiforms are scarce and usually belong to derived species, such as *Carpolestes simpsoni*, *Plesiadapis cookei*, or *Ignacius clarkforkensis* (Bloch and Boyer, 2002; Bloch et al., 2007; Boyer and Gingerich, 2019), that are not representative of the early evolution of this group. However, a recent study carried out on the astragalus and calcaneus of the most basal plesiadapiform, *Purgatorius*, confirms that these animals were arboreal but did not possess a euprimate-like grasp-leaping behavior (Chester et al., 2015). Instead, they are viewed as arboreal clawed-climbers similar to the living scandentian *Ptilocercus lowi*, which is also regarded as a good analogue for the ancestral euarchontan (Szalay and Dagosto, 1988; Sargis, 2002, 2004; Nyakatura, 2019). A remarkable exception is *C. simpsoni*, whose partial skeleton displays euprimate-like hallucal grasping features (Bloch and Boyer, 2002). The transition from an archaic primate to the ancestral euprimate is marked by a substantial increase in the proximodistal elongation of the navicular bone (extensive to the whole midtarsal region), together with the acquisition of a more ovoid proximal facet as well as the rearrangement of the cuneiform and cuboid facets, allowing the foot to engage in more complex rotational movements at the astragalonavicular joint and reducing the mediolateral translation of the foot (Szalay and Decker, 1974; Szalay and Drawhorn, 1980; Dagosto, 1988, 2007). These profound morphological changes explain the major shifts that occurred early in primate evolution, during the radiation of plesiadapiforms and in the branch leading to the ancestral euprimate (Fig. 6; SOM Fig. S7).

The acquisition of a tarsi-fulcrumating foot by the ancestral euprimate, presumably as an adaptation to access the fine-branch milieu, would have led to proximodistal elongation of the midtarsal region to compensate for the decreased load arm, followed by a rapid diversification of locomotor behaviors (Morton, 1924). Omomyiforms retained a small body size and an active arboreal locomotor behavior for which cheirogaleids, particularly the agile *Microcebus* and *Mirza* rather than the more cautious *Cheirogaleus*, might be good analogues (Gebo et al., 1991, 2012, 2015; Anemone and Covert, 2000; Rose et al., 2011). Omomyiforms show lower evolutionary rates than adapiforms, which experienced a body size increase that led to the acquisition of a different type of locomotion than the ancestral euprimate, arguably emphasizing above-branch quadrupedalism, as in extant lemurids (Rose and Walker, 1985; Covert, 1988; Gebo et al., 1991). Some adapiforms, such as the small-bodied *A. frontanyensis*, converged toward the omomyiform condition by displaying a more proximodistally elongated navicular as a result of more active arboreal locomotor behaviors (Marigó et al., 2016, 2020).

5. Conclusions

Our study demonstrates that navicular shape is a reliable indicator of the locomotor behavior in primates and can be used as a predictor to infer the locomotor adaptations of extinct species. Most notably, proximodistal elongation of this bone is related to leaping proclivity, although type of foot posture needs to be considered, as it can influence navicular morphology. Our research also shows that early euprimates displayed a diverse array of locomotor adaptations early on their evolution, although they did not reach the level of specialization displayed by some living groups. Finally, we have assessed the archaic primate—euprimate transition by studying the morphological changes occurred in the navicular bone. Initial increases in navicular elongation, as well as other morphological features such as an ovoid astragalar facet, might be related to the acquisition of a tarsi-fulcrumating foot type and a euprimate-like hallucal grasping, indicating a shift toward a more active locomotor behavior. Collectively, our results provide evidence that early euprimates emerged from a small and unspecialized grasp-leaper animal, but soon diversified into a broad range of locomotor behaviors that allowed the occupation of different arboreal niches.

Acknowledgments

This work has been supported by CERCA Programme/Generalitat de Catalunya, research projects PID2020-116908GB-I00 and PID2020-117289GB-I00 financed by MCIN/AEI/10.13039/501100011033, and project CLT_2022_EXP_ARQ001SOLC_00000197 financed by the Culture Department of the Generalitat de Catalunya, as well as the consolidated research groups 2022 SGR 01188 and 2022 SGR 00620 (Generalitat de Catalunya), Ramón y Cajal grant (RYC2021-034366-I to J.M.) funded by MCIN/AEI/10.13039/501100011033 and by the European Union NextGenerationEU/PRTR, FI AGAUR fellowship (2021 FI_B 00524 and 2022 FI_B1 00131 to O.M.G.) funded by the Secretaria d'Universitats i Recerca de la Generalitat de Catalunya and the European Social Fund. We want to thank our colleagues Doug M. Boyer and Stephen G. B. Chester for providing insightful comments and suggestions that greatly improved an earlier version of the manuscript. We thank Julien Clavel for providing the script for the discriminant analysis. We thank the team of the online repository Morphosource and the following US institutions for providing access to specimens: Museum of Natural History (NY), Duke Lemur Center Division of Fossil Primates (NC), National Museum of Natural History (Washington DC), University of California, Berkeley Museum of Paleontology (CA), University of Michigan Museum of Paleontology (MI), University of Wyoming (WY), and Stony Brook University (NY). We also thank the Leakey Foundation General Research Grant (to Stephen G. B. Chester). This article is part of the Ph.D. dissertation of O.M.G. within the Geology Ph.D. program of the Universitat Autònoma de Barcelona.

Author contributions

O.M.G., A.-C.F., and J.M. designed the research; O.M.G., A. D., A.-C.F., and J.M. carried out the research; O.M.G. and J.M. performed data collection; O.M.G., A.-C.F., and J.M. analyzed the data; and O.M.G., D.M.A., A.-C.F., and J.M. wrote the paper.

Supplementary Online Material

Supplementary Online Material to this article can be found online at https://doi.org/10.1016/j.jhevol.2023.103395.

References

Adams, D.C., Otárola-Castillo, E., 2013. Geomorph: An r package for the collection and analysis of geometric morphometric shape data. Methods Ecol. Evol. 4, 393–399. https://doi.org/10.1111/2041-210X.12035.

Adler, D., Murdoch, D., 2020. Rgl: 3D visualization using openGL. https://github.com/dmurdoch/rgl. https://dmurdoch.github.io/rgl/.

Alfaro, M.E., Bolnick, D.I., Wainwright, P.C., 2005. Evolutionary consequences of many-to-one mapping of jaw morphology to mechanics in labrid fishes. Am. Nat. 165, E140–E154. https://doi.org/10.1086/429564.

Anemone, R.L., Covert, H.H., 2000. New skeletal remains of *Omomys* (Primates, Omomyidae): Functional morphology of the hindlimb and locomotor behavior of a Middle Eocene primate. J. Hum. Evol. 38, 607–633. https://doi.org/10.1006/jhev.1999.0371.

Ankel-Simons, F., 2007. Primate Anatomy, 3rd ed. Academic Press, Burlington.

Arnold, C., Matthews, L.J., Nunn, C.L., 2010. The 10kTrees website: A new online resource for primate phylogeny. Evol. Anthropol. 19, 114–118. https://doi.org/10.1002/evan.20251.

Beard, K.C., Dagosto, M., Gebo, D.L., Godinot, M., 1988. Interrelationships among primate higher taxa. Nature 331, 712–714. https://doi.org/10.1038/331712a0.

Bloch, J.I., Boyer, D.M., 2002. Grasping primate origins. Science 298, 1606–1610. https://doi.org/10.1126/science.1078249.

Bloch, J.I., Silcox, M.T., Boyer, D.M., Sargis, E.J., 2007. New Paleocene skeletons and the relationship of plesiadapiforms to crown-clade primates. Proc. Natl. Acad. Sci. USA 104, 1159–1164. https://doi.org/10.1073/pnas.0610579104.

Bookstein, F.L., Gunz, P., Mitterœcker, P., Mitteroecker, P., Prossinger, H., Schaefer, K., Horst, S., 2003. Cranial integration in *Homo*: Singular warps analysis of the midsagittal plane in ontogeny and evolution. J. Hum. Evol. 44, 167–187. https://doi.org/10.1016/S0047-2484(02)00201-4.

Boyer, D.M., Gingerich, P.D., 2019. Skeleton of late Paleocene *Plesiadapis cookei* (Mammalia, Euarchonta): life history, locomotion, and phylogenetic relationships. Univ. Michigan Pap. Paleontol. 38, 1–269.

Boyer, D.M., Seiffert, E.R., Gladman, J.T., Bloch, J.I., 2013. Evolution and allometry of calcaneal elongation in living and extinct primates. PLoS One 8, e67792. https://doi.org/10.1371/journal.pone.0067792.

Boyer, D.M., Yapuncich, G.S., Butler, J.E., Dunn, R.H., Seiffert, E.R., 2015. Evolution of postural diversity in primates as reflected by the size and shape of the medial tibial facet of the talus. Am. J. Phys. Anthropol. 157, 134–177. https://doi.org/10.1002/ajpa.22702.

Boyer, D.M., Toussaint, S., Godinot, M., 2017a. Postcrania of the most primitive euprimate and implications for primate origins. J. Hum. Evol. 111, 202–211. https://doi.org/10.1016/j.jhevol.2017.07.005.

Boyer, D.M., Gunnell, G.F., Kaufman, S., McGeary, T.M., 2017b. Morphosource: Archiving and sharing 3-d digital specimen data. Paleontol. Soc. Pap. 22, 157–181. https://doi.org/10.1017/scs.2017.13.

Boyer, D.M., Yapuncich, G.S., Dunham, N.T., McNamara, A., Shapiro, L.J., Hieronymus, T.L., Young, J.W., 2019. My branch is your branch: Talar morphology correlates with relative substrate size in platyrrhines at Tiputini Biodiversity Station, Ecuador. J. Hum. Evol. 133, 23–31. https://doi.org/10.1016/j.jhevol.2019.05.012.

Cartmill, M., 1974. Rethinking primate origins. Science 184, 14–21. https://doi.org/10.1126/science.184.4135.436.

Cartmill, M., 1992. New views on primate origins. Evol. Anthropol. 1, 105–111. https://doi.org/10.1002/evan.1360010308.

Castiglione, S., Serio, C., Tamagnini, D., Melchionna, M., Mondanaro, A., Di Febbraro, M., Profico, A., Piras, P., Barattolo, F., Raia, P., 2019. A new, fast method to search for morphological convergence with shape data. PLoS One 14, e0226949. https://doi.org/10.1371/journal.pone.0226949.

Chester, S.G.B., Bloch, J.I., Boyer, D.M., Clemens, W.A., 2015. Oldest known euarchontan tarsals and affinities of Paleocene *Purgatorius* to primates. Proc. Natl. Acad. Sci. USA 112, 1487–1492. https://doi.org/10.1073/pnas.1421707112.

Clavel, J., Escarguel, G., Merceron, G., 2015. mvMORPH: An R package for fitting multivariate evolutionary models to morphometric data. Methods Ecol. Evol. 6, 1311–1319. https://doi.org/10.1111/2041-210X.12420.

Clavel, J., Aristide, L., Morlon, H., 2019. A penalized likelihood framework for high-dimensional phylogenetic comparative methods and an application to new-world monkeys brain evolution. Syst. Biol. 68, 93–116. https://doi.org/10.1093/sysbio/syy045.

Clavel, J., Morlon, H., 2020. Reliable phylogenetic regressions for multivariate comparative data: Illustration with the MANOVA and application to the effect of diet on mandible morphology in phyllostomid bats. Syst. Biol. 69, 927–943. https://doi.org/10.1093/sysbio/syaa010.

Conroy, G.C., Rose, M.D., 1983. The evolution of the primate foot from the earliest primates to the Miocene hominoids. Foot Ankle 3, 342–364. https://doi.org/10.1177/107110078300300604.

Covert, H.H., 1988. Ankle and foot morphology of *Cantius mckennai*: Adaptations and phylogenetic implications. J. Hum. Evol. 17, 57–70. https://doi.org/10.1016/0047-2484(88)90049-8.

Crompton, R.H., Lieberman, S.S., Oxnard, C.E., 1987. Morphometrics and niche metrics in prosimian locomotion: An approach to measuring locomotion, habitat, and diet. Am. J. Phys. Anthropol. 73, 149–177. https://doi.org/10.1002/ajpa.1330730203.

Dagosto, M., 1985. The distal tibia of primates with special reference to the Omomyidae. Int. J. Primatol. 6, 45–75. https://doi.org/10.1007/BF02693696.

Dagosto, M., 1988. Implications of postcranial evidence for the origin of euprimates. J. Hum. Evol. 17, 35–56. https://doi.org/10.1016/0047-2484(88)90048-6.

Dagosto, M., 2007. The postcranial morphotype of primates. In: Ravosa, M.J., Dagosto, M. (Eds.), Primate Origins: Adaptations and Evolution. Springer US, Boston, pp. 489–534. https://doi.org/10.1007/978-0-387-33507-0_15.

Dagosto, M., Marivaux, L., Gebo, D.L., Beard, K.C., Chaimanee, Y., Jaeger, J.-J., Marandat, B., Soe, A.N., Kyaw, A.A., 2010. The phylogenetic affinities of the Pondaung tali. Am. J. Phys. Anthropol. 143, 223–234. https://doi.org/10.1002/ajpa.21308.

Decker, R.L., Szalay, F.S., 1974. Origins and function of the pes in the Eocene Adapidae (Lemuriformes, Primates). In: Jenkins, F.A. (Ed.), Primate Locomotion. Academic Press, New York, pp. 261–291. https://doi.org/10.1016/B978-0-12-384050-9.50014-3.

Demes, B., Günther, M.M., 1989. Biomechanics and allometric scaling in primate locomotion and morphology. Folia Primatol. 53, 125–141. https://doi.org/10.1159/000156412.

Demes, B., Jungers, W.L., Fleagle, J.G., Wunderlich, R.E., Richmond, B.G., Lemelin, P., 1996. Body size and leaping kinematics in Malagasy vertical clingers and leapers. J. Hum. Evol. 31, 367–388. https://doi.org/10.1006/jhev.1996.0066.

Demes, B., Fleagle, J.G., Jungers, W.L., 1999. Takeoff and landing forces of leaping strepsirhine primates. J. Hum. Evol. 37, 279–292. https://doi.org/10.1006/jhev.1999.0311.

Dunn, R.H., 2010. Additional postcranial remains of omomyid primates from the Uinta Formation, Utah and implications for the locomotor behavior of large-bodied omomyids. J. Hum. Evol. 58, 406–417. https://doi.org/10.1016/j.jhevol.2010.02.010.

Dunn, R.H., Sybalsky, J.M., Conroy, G.C., Rasmussen, D.T., 2006. Hindlimb adaptations in *Ourayia* and *Chipetaia*, relatively large-bodied omomyine primates from the Middle Eocene of Utah. Am. J. Phys. Anthropol. 131, 303–310. https://doi.org/10.1002/ajpa.20407.

Fleagle, J.G., 2013. Primate Adaptation and Evolution, 3rd ed. Academic Press, San Diego. https://doi.org/10.1016/B978-0-12-378632-6.00005-7.

Gebo, D.L., 1985. The nature of the primate grasping foot. Am. J. Phys. Anthropol. 67, 269–277. https://doi.org/10.1002/ajpa.1330670312.

Gebo, D.L., 1986. Anthropoid origins—The foot evidence. J. Hum. Evol. 15, 421–430. https://doi.org/10.1016/S0047-2484(86)80025-2.

Gebo, D.L., 1987a. Locomotor diversity in prosimian primates. Am. J. Primatol. 13, 271–281. https://doi.org/10.1002/ajp.1350130305.

Gebo, D.L., 1987b. Functional anatomy of the tarsier foot. Am. J. Phys. Anthropol. 73, 9–31. https://doi.org/10.1002/ajpa.1330730103.

Gebo, D.L., 1988. Foot morphology and locomotor adaptation in Eocene primates. Folia Primatol. 50, 3–41. https://doi.org/10.1159/000156332.

Gebo, D.L., 1989. Postcranial adaptation and evolution in Lorisidae. Primates 30, 347–367. https://doi.org/10.1007/BF02381259.

Gebo, D.L., Dagosto, M., 1988. Foot anatomy, climbing, and the origin of the Indriidae. J. Hum. Evol. 17, 135–154. https://doi.org/10.1016/0047-2484(88)90052-8.

Gebo, D.L., Dagosto, M., Rose, K.D., 1991. Foot morphology and evolution in early Eocene *Cantius*. Am. J. Phys. Anthropol. 86, 51–73. https://doi.org/10.1002/ajpa.1330860105.

Gebo, D.L., Dagosto, M., Beard, K.C., Qi, T., Wang, J., 2000. The oldest known anthropoid postcranial fossils and the early evolution of higher primates. Nature 404, 276–278. https://doi.org/10.1038/35005066.

Gebo, D.L., Dagosto, M., Beard, K.C., Qi, T., 2001. Middle Eocene primate tarsals from China: Implications for haplorhine evolution. Am. J. Phys. Anthropol. 116, 83–107. https://doi.org/10.1002/ajpa.1105.

Gebo, D.L., Smith, T., Dagosto, M., 2012. New postcranial elements for the earliest Eocene fossil primate *Teilhardina belgica*. J. Hum. Evol. 63, 205–218. https://doi.org/10.1016/j.jhevol.2012.03.010.

Gebo, D.L., Smith, R., Dagosto, M., Smith, T., 2015. Additional postcranial elements of *Teilhardina belgica*: The oldest European primate. Am. J. Phys. Anthropol. 156, 388–406. https://doi.org/10.1002/ajpa.22664.

Gelman, A., Rubin, D.B., 1992. Inference from iterative simulation using multiple sequences. Stat. Sci. 7, 457–511. https://doi.org/10.1214/ss/1177011136.

Gladman, J.T., Boyer, D.M., Simons, E.L., Seiffert, E.R., 2013. A calcaneus attributable to the primitive late Eocene anthropoid *Proteopithecus sylviae*: Phenetic affinities and phylogenetic implications. Am. J. Phys. Anthropol. 151, 372–397. https://doi.org/10.1002/ajpa.22266.

Godinot, M., Dagosto, M., 1983. The astragalus of *Necrolemur* (Primates, Microchoerinae). J. Paleontol. 57, 1321–1324.

Goodall, C., 1991. Procrustes methods in the statistical analysis of shape. J. R. Stat. Soc. B Stat. Methodol. 53, 285–339. https://doi.org/10.1111/j.2517-6161.1991.tb01825.x.

Hall-Crags, E.C.B., 1965. An analysis of the jump of the Lesser Galago (*Galago senegalensis*). Proc. Zool. Soc. 147, 20–29. https://doi.org/10.1111/j.1469-7998.1965.tb01874.x.

Hall-Craggs, E.C.B., 1966. Rotational movements in the foot of *Galago senegalensis*. Anat. Rec. 154, 287–293. https://doi.org/10.1002/ar.1091540211.

Hoffstetter, R., 1977. Phylogénie des Primates. Confrontation des résultats obtenus par les diverses voies d'approche du problème. Bull. Mem. Soc. Anthropol. Paris 13, 327–346. https://doi.org/10.3406/bmsap.1977.1886.

Hunt, K.D., Cant, J.G.H., Gebo, D.L., Rose, M.D., Walker, S.E., Youlatos, D., 1996. Standardized descriptions of primate locomotor and postural modes. Primates 37, 363–387. https://doi.org/10.1007/BF02381373.

Lewis, O.J., 1980a. The joints of the evolving foot. Part I. The ankle joint. J. Anat. 130, 527–543.

Lewis, O.J., 1980b. The joints of the evolving foot. Part II. The intrinsic joints. J. Anat. 130, 833–857.
Llera Martín, C.J., Rose, K.D., Sylvester, A.D., 2022. A morphometric analysis of early Eocene Euprimate tarsals from Gujarat, India. J. Hum. Evol. 164, 103141. https://doi.org/10.1016/j.jhevol.2022.103141.
Marigó, J., Minwer-Barakat, R., Moyà-Solà, S., 2011. New *Anchomomys* (Adapoidea, Primates) from the Robiacian (Middle Eocene) of northeastern Spain. Taxonomic and evolutionary implications. J. Hum. Evol. 60, 665–672. https://doi.org/10.1016/j.jhevol.2010.12.006.
Marigó, J., Roig, I., Seiffert, E.R., Moyà-Solà, S., Boyer, D.M., 2016. Astragalar and calcaneal morphology of the middle Eocene primate *Anchomomys frontanyensis* (Anchomomyini): Implications for early primate evolution. J. Hum. Evol. 91, 122—143. https://doi.org/10.1016/j.jhevol.2015.08.011.
Marigó, J., Minwer-Barakat, R., Moyà-Solà, S., Boyer, D.M., 2020. First navicular remains of a European adapiform (*Anchomomys frontanyensis*) from the Middle Eocene of the Eastern Pyrenees (Catalonia, Spain): Implications for early primate locomotor behavior and navicular evolution. J. Hum. Evol. 139, 102708. https://doi.org/10.1016/j.jhevol.2019.102708.
Marivaux, L., Beard, K.C., Chaimanee, Y., Dagosto, M., Gebo, D.L., Guy, F., Marandat, B., Khaing, K., Kyaw, A.A., Oo, M., Sein, C., Soe, A.N., Swe, M., Jaeger, J.-J., 2010. Talar morphology, phylogenetic affinities, and locomotor adaptation of a large-bodied amphipithecid primate from the late middle Eocene of Myanmar. Am. J. Phys. Anthropol. 143, 208–222. https://doi.org/10.1002/ajpa.21307.
Marivaux, L., Tabuce, R., Lebrun, R., Ravel, A., Adaci, M., Mahboubi, M., Bensalah, M., 2011. Talar morphology of azibiids, strepsirhine-related primates from the Eocene of Algeria: Phylogenetic affinities and locomotor adaptation. J. Hum. Evol. 61, 447–457. https://doi.org/10.1016/j.jhevol.2011.05.013.
Mitteroecker, P., Gunz, P., 2009. Advances in geometric morphometrics. Evol. Biol. 36, 235–247. https://doi.org/10.1007/s11692-009-9055-x.
Morton, D.J., 1924. Evolution of the human foot II. Am. J. Phys. Anthropol. 7, 1–52. https://doi.org/10.1002/ajpa.1330070114.
Moyà-Solà, S., Köhler, M., Alba, D.M., Roig, I., 2012. Calcaneal proportions in primates and locomotor inferences in *Anchomomys* and other Palaeogene Euprimates. Swiss J. Palaeontol. 131, 147–159. https://doi.org/10.1007/s13358-011-0032-5.
Napier, J.R., Walker, A.C., 1967. Vertical clinging and leaping — A newly recognized category of locomotor behaviour of primates. Folia Primatol. 6, 204–219. https://doi.org/10.1159/000155079.
Nyakatura, J.A., 2019. Early primate evolution: Insights into the functional significance of grasping from motion analyses of extant mammals. Biol. J. Linn. Soc. 127, 611–631. https://doi.org/10.1093/biolinnean/blz057.
Oxnard, C.E., Crompton, R.H., Lieberman, S.S., 1990. Animal Lifestyles and Anatomies. University of Washington Press, Seattle.
Plummer, M., Best, N., Cowles, K., Vines, K., 2005. CODA: Convergence diagnosis and output analysis for MCMC. R News 6, 7–11.
Qiao, Z., Zhou, L., Huang, J.Z., 2009. Sparse linear discriminant analysis with applications to high dimensional low sample size data. Int. J. Appl. Math. 39, 48–60.
R Core Team, 2022. R: A language and environment for statistical computing. R Foundation for Statistical Computing, Vienna.
Rasmussen, D.T., 1990. Primate origins: Lessons from a neotropical marsupial. Am. J. Primatol. 22, 263–277. https://doi.org/10.1002/ajp.1350220406.
Revell, L.J., 2012. phytools: An R package for phylogenetic comparative biology (and other things). Methods Ecol. Evol. 3, 217–223. https://doi.org/10.1111/j.2041-210X.2011.00169.x.
Rohlf, F.J., Slice, D., 1990. Extensions of the Procrustes method for the optimal superimposition of landmarks. Syst. Zool. 39, 40–59. https://doi.org/10.2307/2992207.
Rohlf, F.J., Corti, M., 2000. Use of two-block partial least-squares to study covariation in shape. Syst. Biol. 49, 740–753. https://doi.org/10.1080/106351500750049806.
Rose, K.D., 1994. The earliest primates. Evol. Anthropol. 3, 159–173. https://doi.org/10.1002/evan.1360030505.
Rose, K.D., Walker, A., 1985. The skeleton of early Eocene *Cantius*, oldest lemuriform primate. Am. J. Phys. Anthropol. 66, 73–89. https://doi.org/10.1002/ajpa.1330660107.
Rose, K.D., Chester, S.G.B., Dunn, R.H., Boyer, D.M., Bloch, J.I., 2011. New fossils of the oldest North American euprimate *Teilhardina brandti* (Omomyidae) from the Paleocene–Eocene thermal maximum. Am. J. Phys. Anthropol. 146, 281–305. https://doi.org/10.1002/ajpa.21579.
Sargis, E., 2002. The postcranial morphology of *Ptilocercus lowii* (Scandentia, Tupaiidae): An analysis of primatomorphan and volitantian characters. J. Mamm. Evol. 9, 137–160. https://doi.org/10.1023/A:1021387928854.
Sargis, E., 2004. New views on tree shrews: The role of tupaiids in primate supraordinal relationships. Evol. Anthropol. 13, 56–66. https://doi.org/10.1002/evan.10131.
Seiffert, E.R., Simons, E.L., 2001. Astragalar morphology of late Eocene anthropoids from the Fayum Depression (Egypt) and the origin of catarrhine primates. J. Hum. Evol. 41, 577–606. https://doi.org/10.1006/jhev.2001.0508.
Seiffert, E.R., Simons, E.L., Clyde, W.C., Rossie, J.B., Attia, Y., Bown, T.M., Chatrath, P., Mathison, M.E., 2005. Basal anthropoids from Egypt and the antiquity of Africa's higher primate radiation. Science 310, 300–304. https://doi.org/10.1126/science.1116569.
Seiffert, E.R., Costeur, L., Boyer, D.M., 2015. Primate tarsal bones from Egerkingen, Switzerland, attributable to the middle Eocene adapiform *Caenopithecus lemuroides*. PeerJ 3, e1036. https://doi.org/10.7717/peerj.1036.
Silcox, M.T., Sargis, E.J., Bloch, J.I., Boyer, D.M., 2015. Primate origins and supraordinal relationships: Morphological evidence. In: Henke, W., Tatterstall, I. (Eds.), Handbook of Paleoanthropology, 2nd ed. Springer, Heidelberg, pp. 1053–1081. https://doi.org/10.1007/978-3-642-39979-4_29.
Silcox, M.T., Bloch, J.I., Boyer, D.M., Chester, S.G.B., López-Torres, S., 2017. The evolutionary radiation of plesiadapiforms. Evol. Anthropol. 26, 74–94. https://doi.org/10.1002/evan.21526.
Su, A., Zeiniger, A., 2022. The primate ankle and hindfoot. In: Zeiniger, A., Hatala, K.G., Wunderlich, R.E., Schmitt, D. (Eds.), The Evolution of the Primate Foot. Anatomy, Function, and Palaeontological Evidence, 1st ed. Springer, Cham, pp. 21–45. https://doi.org/10.1007/978-3-031-06436-4_3.
Sussman, R.W., 1991. Primate origins and the evolution of angiosperms. Am. J. Primatol. 23, 209–223. https://doi.org/10.1002/ajp.1350230402.
Szalay, F.S., Decker, R.L., 1974. Origins, evolution, and function of the tarsus in late Cretaceous Eutheria and Paleocene primates. In: Jenkins, F.A. (Ed.), Primate Locomotion. Academic Press, New York, pp. 223–259. https://doi.org/10.1016/B978-0-12-384050-9.50013-1.
Szalay, F., Dagosto, M., 1980. Locomotor adaptations as reflected on the humerus of Paleogene primates. Folia Primatol. 34, 1–45. https://doi.org/10.1159/000155946.
Szalay, F.S., Drawhorn, G., 1980. Evolution and diversification of the Archonta in an arboreal milieu. In: Luckett, W.P. (Ed.), Comparative Biology and Evolutionary Relationships of Tree Shrews. Springer, Boston, pp. 133–169. https://doi.org/10.1007/978-1-4684-1051-8_4.
Szalay, F.S., Dagosto, M., 1988. Evolution of hallucial grasping in the primates. J. Hum. Evol. 17, 1–33. https://doi.org/10.1016/0047-2484(88)90047-4.
Torres-Tamayo, N., Schlager, S., García-Martínez, D., Sanchis-Gimeno, J.A., Nalla, S., Ogihara, N., Oishi, M., Martelli, S., Bastir, M., 2020. Three-dimensional geometric morphometrics of thorax-pelvis covariation and its potential for predicting the thorax morphology: A case study on Kebara 2 Neandertal. J. Hum. Evol. 147, 102854. https://doi.org/10.1016/j.jhevol.2020.102854.
Wainwright, P.C., Alfaro, M.E., Bolnick, D.I., Hulsey, C.D., 2005. Many-to-one mapping of form to function: A general principle in organismal design? Integr. Comp. Biol. 45, 256–262. https://doi.org/10.1093/icb/45.2.256.
Walker, A., 1974. Locomotor adaptations in past and present prosimian primates. In: Jenkins, F.A. (Ed.), Primate Locomotion. Academic Press, New York, pp. 349–381. https://doi.org/10.1016/B978-0-12-384050-9.50016-7.
Wiley, D., 2006. Landmark Editor 3.0. Institute for Data Analysis and Visualization, University of California, Davis.
Williams, B., Kay, R., Kirk, E., Ross, C., 2010. *Darwinius masillae* is a strepsirrhine—a reply to Franzen et al. (2009). J. Hum. Evol. 59, 567–573. https://doi.org/10.1016/j.jhevol.2010.01.003.
Willmott, C.J., Matsuura, K., 2005. Advantages of the mean absolute error (MAE) over the root mean square error (RMSE) in assessing average model performance. Clim. Res. 30, 79–82. https://doi:10.3354/cr030079.
Yapuncich, G.S., Seiffert, E.R., Boyer, D.M., 2017. Quantification of the position and depth of the *flexor hallucis longus* groove in euarchontans, with implications for the evolution of primate positional behavior. Am. J. Phys. Anthropol. 163, 367–406. https://doi.org/10.1002/ajpa.23213.
Yapuncich, G.S., Feng, H.F., Dunn, R.H., Seiffert, E.R., Boyer, D.M., 2019. Vertical support use and primate origins. Sci. Rep. 9, 12341. https://doi.org/10.1038/s41598-019-48651-x.
Yapuncich, G.S., Chester, S.G.B., Bloch, J.I., Boyer, D.M., 2022. The feet of Paleogene primates. In: Zeiniger, A., Hatala, K.G., Wunderlich, R.E., Schmitt, D. (Eds.), The Evolution of the Primate Foot. Anatomy, Function, and Palaeontological Evidence, 1st ed. Springer, Cham, pp. 277–319. https://doi.org/10.1007/978-3-031-06436-4_12.